



ACTIVITY BOOK FOR STUDENTS

First edition



CONTENTS

1.	Introduction and scope	5
1.1	The EASY System	6
1.2	Getting Connected	7
1.3	Safety precautions	9
2.	Silicon Strip Detectors	11
2.1	Semiconductors: Intrinsic And Extrinsic	11
2.2	P-N Junction	13
2.3	Silicon Micro-strip Detector	16
2.4	Signal Formation	18
2.5	Spatial Resolution	18
2.6	Sources of Noise	19
2.7	Trigger Modes	20
3.	Data Acquisition Program	21
3.1	Downloading Alibava-Gui	21
3.2	Starting Alibava-Gui	21
3.3	Taking Data	23
3.3.1	Calibration Run	23
3.3.2	Laser Synchronization	25
3.3.3	Pedestal Run	26
3.3.4	Laser run	26
3.3.5	Radioactive source run (RS)	26
3.4	Configuring EASY	27
3.4.1	Data File Format	27
3.4.2	DAQ configuration	27
3.4.3	BEETLE configuration	28
3.4.4	External Trigger configuration	29
3.4.5	BEETLE Comparator Configuration	30
3.4.6	Analysis configuration	30
3.4.7	Latency	31
3.4.8	Load and Save Pedestals	31
3.5	Calibration Of The Individual Channel Corrections To The Comparator Threshold	31
3.6	Monitoring The Data	33
3.6.1	Signal tab	34
3.6.2	Event Display tab	34
3.6.3	Noise/Common Noise tab	35
3.6.4	Pedestal tab	35
3.7	Changing Histogram Attributes And Histogram Printing	35
3.8	The HDF5 Data Format	36
4.	Exercises	39
4.1	Setting the Operation Voltage and Detector Current	39
4.2	Pedestal, Electronic Noise And Common Noise	41

4.3	Signal, S/N Rate And Cluster Finding Algorithm.	45
4.4	Diode Trigger Synchronization and Pulse Reconstruction.	48
4.5	Charge Collection and Energy Deposition.	51
4.6	Charge Collection Efficiency (CCE) and Depletion Voltage.	54
4.7	Strip structure and Charge shareing.	56
4.8	Spatial Resolution: Binary vs Analogical Readout.	59
4.9	Laser Penetration in Silicon.	63
4.10	Spectroscopy using Self-Trigger.	65
	Bibliography	69

1. INTRODUCTION AND SCOPE.

The **Alibava Educational System (EASY)** is a complete instrumentation system dedicated to Silicon micro-strip Radiation Detectors, representing the state-of-the-art in detector characterization. It is based on the Alibava System (*ALIBAVA Collaboration*) largely used within the CERN (*CERN*) community to test micro-strip detectors for particle and nuclear physics experiments. The system can be configured to work with laser light or radioactive sources. The set-up is ideal for making basic or complex experiments with silicon micro-strip detectors similar to the ones performed in the actual research field, in facilities such as LHC at CERN, DESY (*DESY*), FERMILAB (*Fermilab*), Synchrotrons, etc. This easy-to-use electronic equipment establishes the basis for an affordable and complete set for student laboratory experiments.

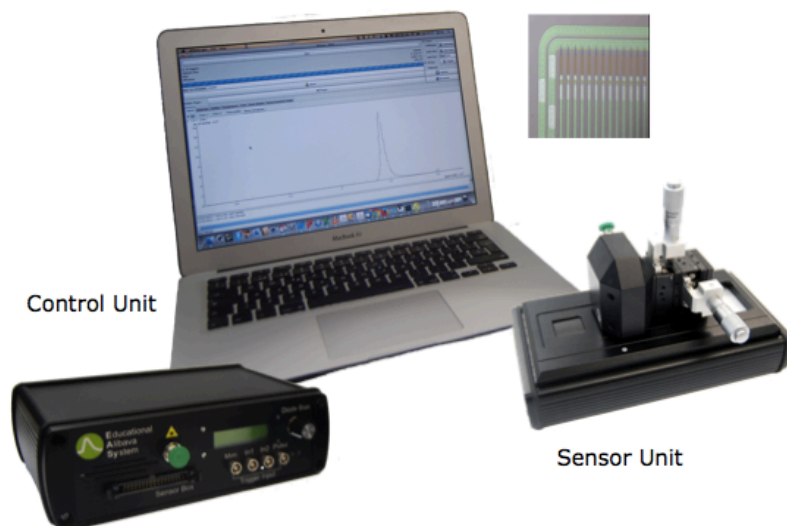


Figure 1.1.- EASY system with the Control Unit, the Sensor Unit and the acquisition program Alibava-gui running in the computer.

The aim of this system is to illustrate the operation of a silicon strip detectors, in particular:

- To observe the noise of a silicon strip detector as a function of bias voltage.

- To observe the signal spectra due to a minimum ionising particle in a silicon detector and demonstrate the Landau distribution shape of collected charge.
- To determinate the Charge Collection efficiency of a silicon detector.
- To observe charge sharing between strip and relate this to the position resolution of the detector.
- To illustrate the structure of a typical micro-strip detector.
- To compare the charge deposition of minimum ionization particles and gamma particles.



Figure 1.2.- Briefcase containing the Control Unit, Sensor Unit, power supply, cables and optic fibre.

1.1 THE EASY SYSTEM

The components of the EASY systems are the **Control Unit** (system's main board) and the **Sensor Unit** (containing the detector board), the full system is shown in Figure 1.1. The Control Unit, Sensor Unit, power supply, cables and optical fibre come in a briefcase (Figure 1.2). The Control Unit is the heart of the system communicating with the sensor unit and the Computer software. Its main characteristics are:

- Xilinx device retained with support chipset
- Plug and play.
- Interface with Sensor Unit via 34 IDC connector.
- Incorporates all control.
- USB 2.0 interface with the computer.
- High Voltage module to supply the detector bias.
- Pulse laser source.
- External input trigger timing and synchronization.

The Sensor Unit incorporates an electronic board, seen in Figure 1.3 to accommodate the BEETLE readout chip (ASIC). This chip provides 128 analogue input channels with 40 MHz clocked analogue pipeline (maximum programmable latency of 4 μ s).

The BEETLE dynamic range is +/- 100.000 electron equivalent charge. The ASIC is connected to a P-on-N silicon sensor. The sensor has 128 strips with 160 μ m pitch and 300 μ m thickness..

The typical depletion voltage of the detector is between 60-80V and the leakage current at full depletion is less than 10 nA/strip.

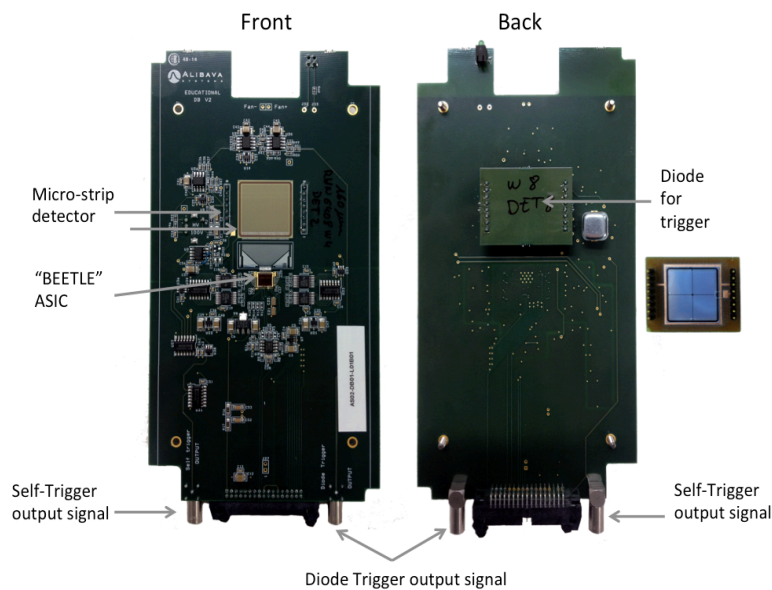


Figure 1.3.- "Sensor Unit holding the micro-strip detector and the BEETLE in the front side and the Diode for trigger proposes in the back. The Board have two connectors for the trigger signal: Diode Trigger and Self-Trigger.

The unit also generates a trigger signal, which is useful to indicate the exact time at which a particle crosses the micro-strip sensor. There are two trigger modes: diode mode and self-trigger mode, described in detail in section 2.7.

The diode trigger mode consists in discriminating a signal generated by a low noise silicon diode. The silicon diode is mounted underneath the micro-strip sensor with a gap of few millimetres. A HV module sitting in the same board powers the diode.

The Beetle chip incorporates a fast comparator for each single channel. The charge collected by the micro-strip sensor and arriving to the chip can generate a self-trigger in the chip using this fast comparator.

The system incorporates a 980nm (5ns pulses width) laser to induce charge in the detector. The laser peak power is 0.6mW and spot around 20 μ m. The laser is hold on the Control Unit and connected to the detector board with an optical fibre.

The system includes a specific data acquisition software and data analysis tools to demonstrate and visualize the operating principles of the silicon strip detector.

1.2 GETTING CONNECTED

The Control Unit front and back panels are displayed in Figure 1.4. The name and function of each component are:

1. Socket for the laser optic fibre connection.
2. Flat cable connector for communication between the Control Unit and the Sensor Unit. Including bias voltage for the micro-strip detector.
3. Display to show bias voltage and sensor leakage current.

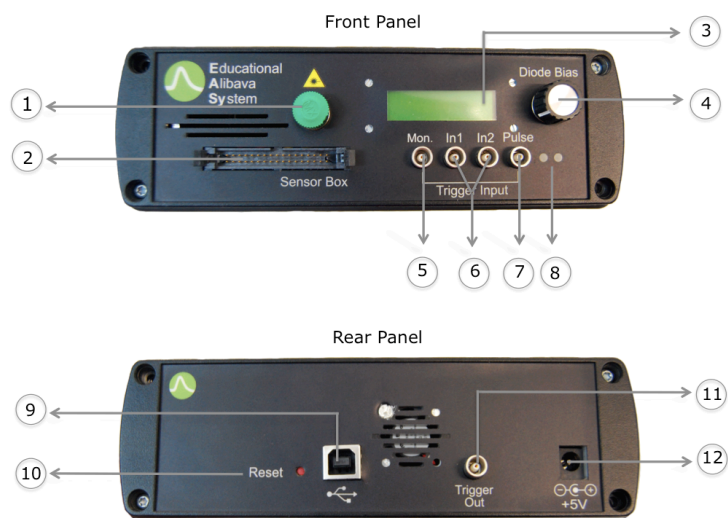


Figure 1.4.- Front and Rear Control Unit panels.

4. Bias voltage supply adjustment.
5. LEMO jack for monitoring the data process by the BEETLE.
6. LEMO jack input for external trigger coincidence (not used in these exercises).
7. LEMO jack input for the single trigger signal (from Diode or Self trigger).
8. On/Off and trigger led indicators.
9. USB jack for connection to the computer.
10. Manual Reset button.
11. LEMO jack input external laser trigger (not used in these exercises) or to monitor the laser shot.
12. Power supply (+5V).

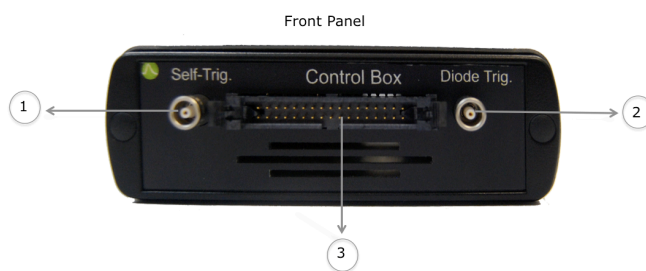


Figure 1.5.- Front Sensor Unit box.

Figure 1.5 shows the front panel of the Sensor Unit, with the following names and functions:

1. LEMO jack output to provide the self-trigger signal.
2. LEMO jack output to provide the Diode trigger signal.
3. Flat cable connector for communication between the Control Unit and the Sensor Unit.

To operate the system, the connections needed between the Control Unit and the Sensor Unit (Figure 1.6) comprise:

- Flat cable between (2) of the Control Unit and (2) of the Control Unit.
- LEMO cable between (7) of the Control Unit and (1) or (3) of the Sensor Unit depending on the trigger used.
- Optical fibre between the top of the Sensor Unit and (1) of the Control Unit.

The Sensor Unit has a mobile part that slides over the box walls. It has two positions: Radioactive source position and Laser position (Figure 1.7). Depending on the data acquisition considered the user will choose one of these positions.

With the Radioactive source position the user will place the radioactive source on the carbon fibre rectangle (radioactive source receptacle). This receptacle is aligned with the micro-strip sensor. When Laser position is used, the Laser beam will be align with the micro-strip sensor. The two micro-positioners screws (Figure 1.6) allow to movement of the laser lent in 10µm steps, horizontally and vertically, to focus the laser and to move the laser beam over the sensor.

Finally, the system has to be powered using the power adapter provided with the system, and connected to the

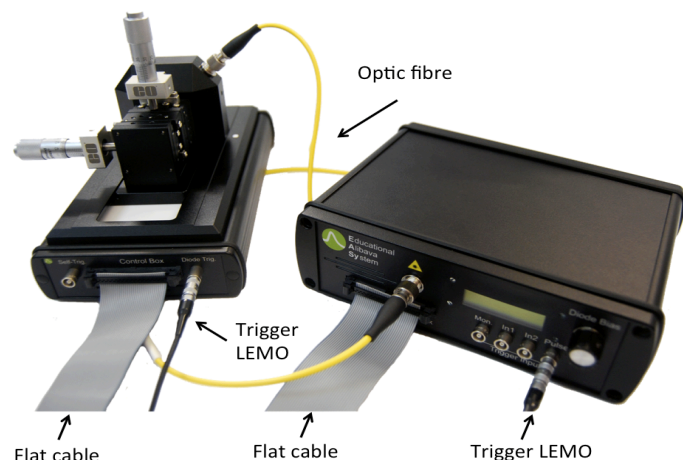


Figure 1.6.- Connections between the Control Unit and the Sensor Unit.

computer using the USB cable between the Computer and USB jack of the Control Unit (9).

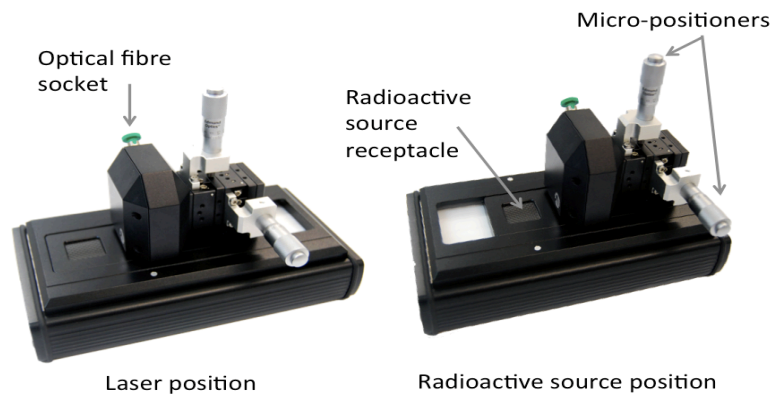


Figure 1.7.-Sensor Unit position for data acquisition (Radioactive source and Laser).

1.3 SAFETY PRECAUTIONS.

Please read the safety precautions carefully to ensure the correct use of EASY system:

Do not open the Sensor or Control Unit.

Please use the flat cable safety lock tabs properly, do not force them.

Do not remove the carbon fibre of the Sensor Unit.

Do not bend the flat cable.

EASY employs class 1 laser. The class 1 laser is safe under all conditions of normal use. This means the maximum permissible exposure (MPE) cannot be exceeded in that condition. It must not be opened without shutting down the laser (the laser is only shuttled during the laser data acquisition and laser calibration). To prevent direct exposure to the laser beam, stop the data acquisition while connecting the optic fibre to the units. Avoid direct eye exposure to the laser beam.



2. SILICON STRIP DETECTORS.

2.1 SEMICONDUCTORS: INTRINSIC AND EXTRINSIC.

Semiconductors are a special class of material with properties between those of insulators and conductors (*Kittel*). Since their resistivity values are in between those types of material (in the order of 1×10^{-6} ohm-metres for conductors and in the order of 1×10^{13} ohm-metres for insulators), they are neither good conductors nor good insulators. The electrical conductivity in a semiconductor can be controlled by doping, i.e. adding impurities. The material is characterised by an energy band diagram with an energy gap between the conduction and valence bands of a few electron volts (for more than 4eV the

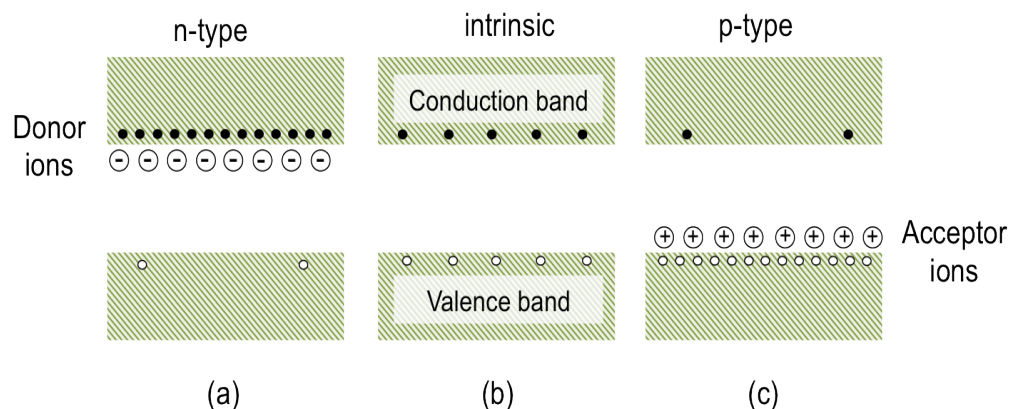


Figure 2.1.- Schematic energy band representation of extrinsic n-type (a), intrinsic (b) and extrinsic p-type (c) semiconductors.

material is said to be an insulator). The current in a semiconductor is carried by a flow of electrons and or by positively charged particles called 'holes' in the electron structure of the material. The electrons are free to conduct (known as free electrons) when they inhabit the conduction band. This takes place due to thermal excitation or doping. When an electron is excited from the valence band to the conduction band it leaves behind a

hole in the valence band, which can be treated as a charge carrier with positive charge (Figure 2.1.b).

The conductivity of the material is controlled by the impurity concentration. Intrinsic semiconductors contain no impurities (in practice, very few). Silicon is a group IV element with four valence electrons. Doping with a group V material (with 5 valence electrons) introduces an extra electron into the crystal structure, which inhabits the conduction band. This is known as n-type doped material (extrinsic n-type material). Similarly doping with a group III element (three valence electrons) introduces a lack of an electron, or a hole, into the material. This is known as p-type doped material (extrinsic p-type material). Figure 2.2.a shows a two-dimensional schematic representation of a silicon crystal with a silicon atom replaced by an arsenic atom with five valence electrons. Only four electrons are used for the formation of the covalent bonds with the neighbouring atoms, while the fifth electron is not bound to a specific atom and it is free for conduction. If a silicon atom is replaced by an atom with only three valence electrons (Figure 2.2.b) one electron is missing in the covalent bonds and a hole is thus created. This hole may be filled by an electron from a neighbouring atom, this being equivalent to a movement of the hole (positive charge). From the point of view of the band model, the replacement of a proper atom of the silicon lattice by a different atom is accompanied by the creation of localized energy levels in the band gap. These energy levels may be of the

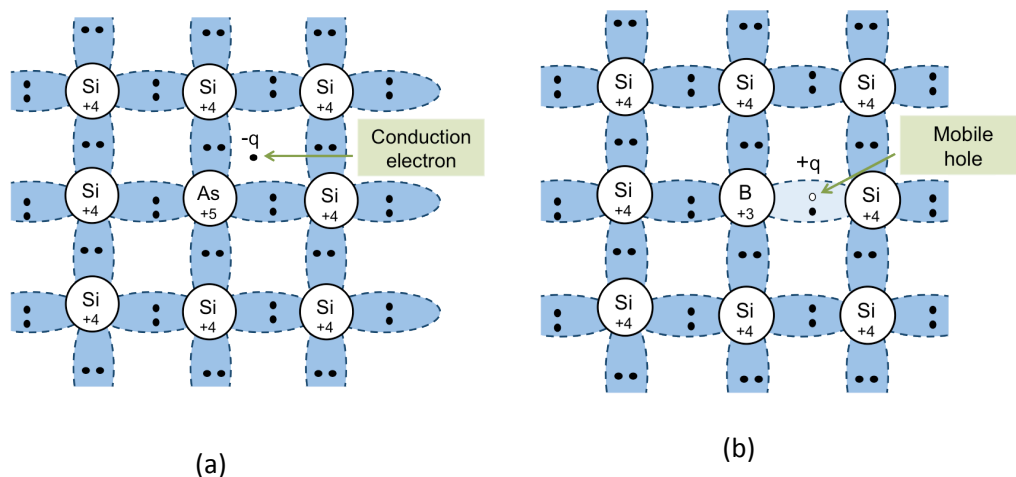


Figure 2.2.- Covalence bond representation of n-type (a) and p-type (b) extrinsic semiconductor.

donor or acceptor type. If the donor levels are close to the conduction band (as is the case of the silicon doped with arsenic), the electrons will be transported to the conduction band (Figure 2.1.a) at room temperature. Equivalent considerations hold for acceptor-type states as boron in silicon. These states will be filled almost completely and holes will be .d in the valence band (Figure 2.1.c).

In an intrinsic semiconductor, electron-hole pairs are continuously being generated by thermal energy. At the same time, there is also a certain number of electrons and holes that recombine. Under stable conditions an equilibrium concentration of electrons-hole pairs n_i is established. When an external electrical field is applied, the drift velocity of the electrons and holes through a semiconductor can be written as:

$$\begin{aligned} v_e &= \mu_e E \\ v_h &= \mu_h E \end{aligned} \quad (1)$$

where E is the magnitude of the electric field and μ_e and μ_h are the mobilities of the electrons and holes respectively. The mobilities determine the current in a semiconductor. Since the current density $J = \rho v$, where ρ is the charge density and v the velocity, J in pure semiconductor is given by:

$$J = e n_i (\mu_e + \mu_h) E \quad (2)$$

Notice that both electrons and holes carry the current. Carrier transport is due to drift (with drift velocities of equation (1)) and also to diffusion. Diffusion is due to random thermal motion that tends to smooth a non-uniform carrier distribution. Diffusion D and mobility μ , are related by the Einstein relation:

$$D = \frac{kT}{q} \mu \quad (3)$$

2.2 P-N JUNCTION.

A simple diode structure, called a p-n junction, is formed when a piece of p-type and a piece of n-type doped material are brought together. In the p-n junction electrons diffuse, due to the carrier concentration difference, from the n-type material to the p-type material leaving a net positive fixed charge in the n-type region. The electrons recombine with the holes in the p-type material. Likewise, free holes diffuse from the p-type material to the n-type, recombining with electrons, leaving a region of negative fixed charge in the p-type material. The fixed positive charge causes a force on the charge carriers and creates a drift. The region of fixed space charge is known as the depletion region as it is depleted (free of) mobile charge carriers. The width of the depletion zone is generally small and depends on the concentration of doping of n and p impurities (group V and group III atoms). Due to the fixed charge a potential is present over the depletion region, and therefore an electric field exists. The principle of the p-n junctions is shown in Figure 2.3.

Because its electric field configuration, the depletion layer also has a certain capacitance width, as we will see later, it affects the noise when the junction is used as a detector. For a planar geometry, the capacitance is:

$$C = \epsilon \frac{A}{d} \quad (4)$$

where A is the area of the depletion zone, d its width and ϵ the silicon dielectric constant.

The application of a reverse bias (V) over the p-n junction (negative voltage is applied to the p-type side and a positive voltage to the n-type side) has the effect of attracting the holes in the p-region away from the junction and towards the p contact and similarly for the electrons in the n-region. The net effect is to enlarge the depletion zone, the higher V is, the wider the depletion zone. The depletion region grows with V and eventually the material will become fully depleted, i.e. leading to a region free of charges. At some point, the junction will breakdown and begin conducting (Figure 2.4).

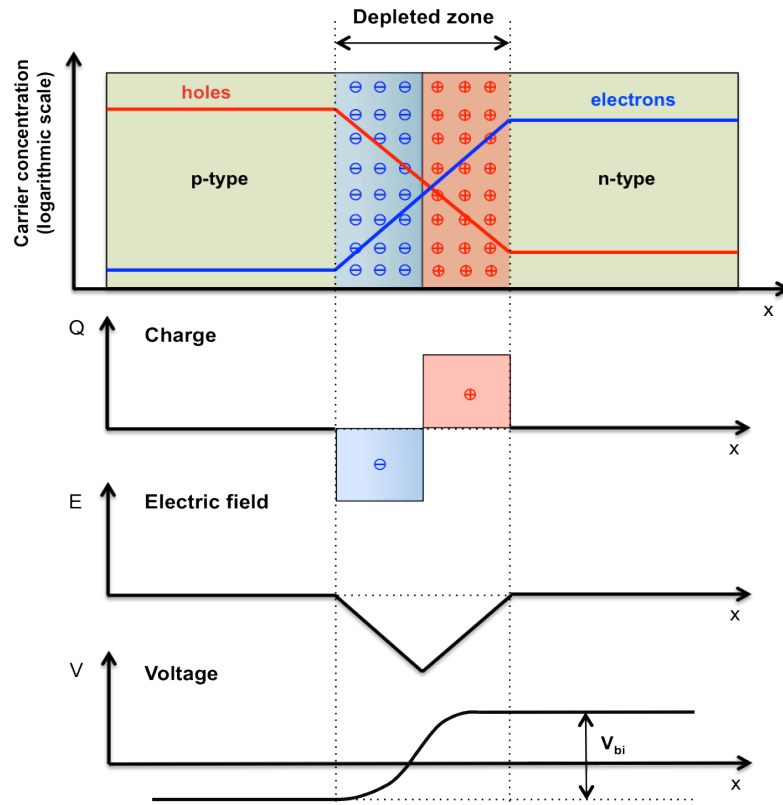


Figure 2.3.- Diagram of the interface region of a p-n junction, each diagram shows a variable as a function of distance: the p-type and n-type silicon with the free charge carriers concentration with holes in the p-type side and electrons in the n-type one (note the depletion of carriers in the depletion region), the fixed space charge density (Q), the electric field (E) and the building-in voltage (V_{bi}).

The width of the depletion region increases with V according with the equation:

$$d = \sqrt{\frac{2 \varepsilon (V_{bi} + V)}{q N_{eff}}} \quad (5)$$

where V_{bi} is the building-in voltage (Figure 2.3) and N_{eff} is the doping effective concentration given by :

$$N_{eff} = \frac{N_D N_A}{N_D + N_A} \quad (6)$$

N_D and N_A being the impurity concentration of donor and acceptor respectively. Capacitance can be calculated as a function of external voltage,

$$C = \sqrt{\frac{q N_{eff} \varepsilon}{2(V_{bi} + V)}} \quad (7)$$

Typically $V \gg V_{bi}$, hence V_{bi} is commonly neglected. Equation (7) is valid up to reach

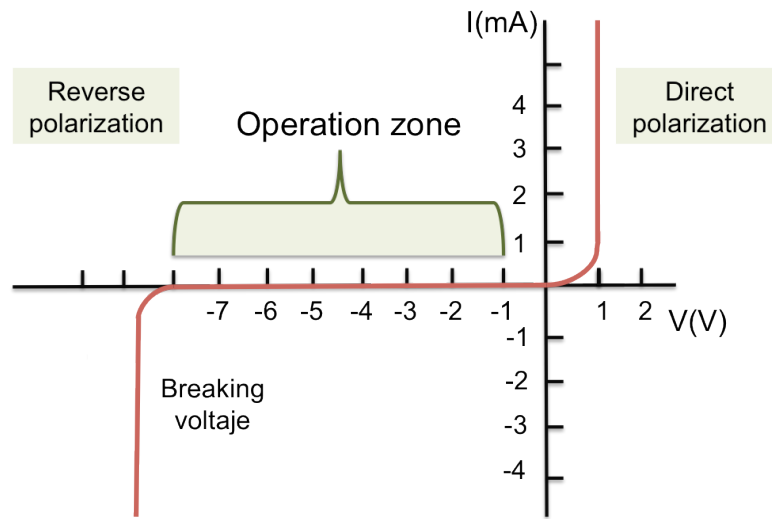


Figure 2.4.- Ideal current-voltage characteristics of a p-n junction.

full depletion ($V=V_{dep}$). For larger external voltage ($V>V_{dep}$), capacitance C remains constant, as the depletion width cannot increase, ie, for $V=V_{dep}$ the depletion region extends over the full semiconductor thickness. Thereby, the depletion voltage V_{dep} can be determined from the capacitance. It is worth noting that the higher the resistivity of the material, the lower the necessary bias voltage is to fully deplete a given thickness.

The depletion voltage can be calculated from equation (5) for a detector of thickness D ,

$$V_{dep} \approx \frac{q}{2\epsilon} N_{eff} D^2 \quad (8)$$

If $V > V_{dep}$, the electric field can be considered approximately constant. When the applied voltage is below full depletion, the field does not extend over the whole bulk. With its maximum still at the junction, only a fraction of the sensor is depleted. Consequently, the charge collection is inefficient in that case, since the carriers do not move outside the electric field. The width of the depletion zone, d_c , is given by,

$$d_c = D \sqrt{\frac{V}{V_{dep}}} \quad (9)$$

Thus, the efficiency of a silicon detector is given by

$$\begin{aligned} \sqrt{V/V_{dep}} & \quad \text{for} \quad 0 \leq V \leq V_{dep} \\ 1 & \quad \text{for} \quad V > V_{dep} \end{aligned} \quad (10)$$

If an external electric potential with the opposite sign to V_{bi} is applied to the detector, the p-n junction is said to be direct polarized. The barrier for electrons moving from n- to p-side is decreased. The current flow in this direction increases exponentially (see Figure 2.4), not being suitable for particle detection.

When a silicon detector operates under reverse bias conditions, the resulting current is called the leakage current. The current that flows through a p-n junction has several components, namely; the diffusion current through the barrier (reverse current), generation currents in the space charge region, surface current, and currents associated

with the edge of the device.

2.3 SILICON MICRO-STRIP DETECTOR.

Silicon detectors are constructed with one or several P-N junctions. Starting from a planar structure of doped silicon, traditionally n type, one of the surfaces is doped with the opposite type, traditionally p type. As the thickness of this surface doping is small compared to the structure bulk, the doping concentration is higher. A silicon micro-strip detector is build segmenting the top layer in strips (Figure 2.5). A full description of silicon detector can be found in (Leo) and (Lutz).

EASY system uses a p-on-n sensor, the same type of sensor used in ATLAS detector at LHC. P-on-n strip detectors consist typically of an around 300 μ m thick n-type bulk. On one side, a thin layer segments form strips out of p-type material, whereas the back implant is n+. The abrupt junctions are formed between the strips and the bulk silicon. The depletion zone grows from the strips to the backplane so that, the device can operate partially depleted and the movement of holes forms the signal. Figure 2.5 shows the sketch of our sensor.

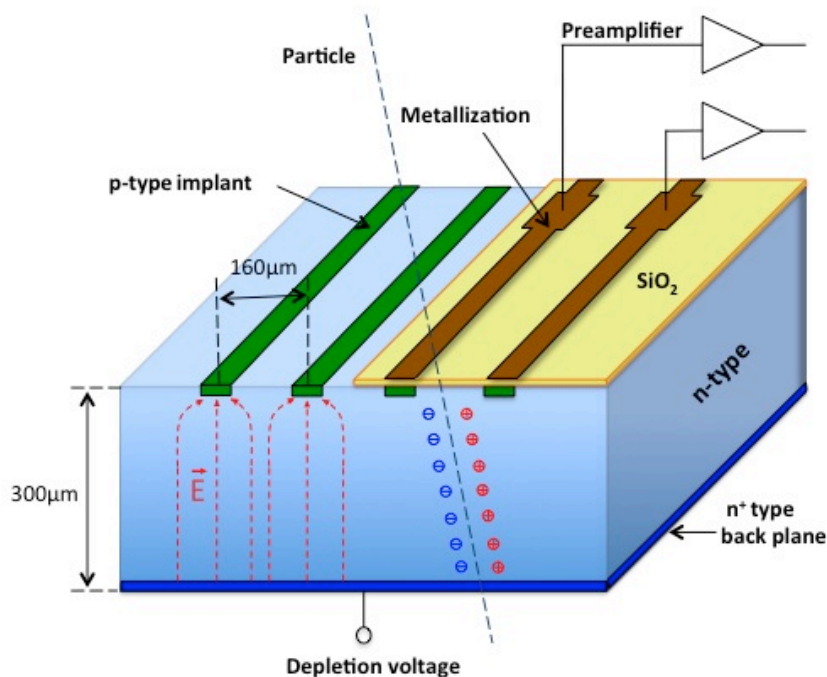


Figure 2.5.- Sketch of the EASY micro-strip p-on-n silicon detector.

In addition, other elements are necessary to build a proper silicon detector:

- An oxide layer (approximately 1-4 μ m thick) lies on top of the implanted strips, known as the AC oxide, which prevents the leakage current flowing directly to the readout electronics.
- The signal from each of the strips is capacitive coupled (AC) to a metal strip (Al) lying directly above the p strip implants, and the charge is read out through this ohmic contact.
- In order to bias the implant strips in the front side, a common bias rail (Figure 2.6)

runs at the edge of the sensor and is connected to each strip via a resistor, a polysilicon bias resistor is used in EASy.

- A low resistance ohmic contact to the back of the device is required for applying the high voltage and is obtained through an n+ implant with a layer of metal in direct contact that covers the entire backside of the device. The n+ implant is required to prevent the depletion region reaching the metallisation.
- The guard ring structure is a feature specifically made to minimise the leakage current at the detector edges and avoid possible electrical breakdown. Outside the sensitive region of the device, the situation is a bit more complex as not the whole surface is at the same potential. The cutting edge is conductive due to mechanical damage caused by the cutting procedure and could be at the backplane potential, which is the bias voltage. Due to the lateral extension of the depletion, when the space charge reaches the cutting edge the strong crystal damage that is present there, acts as a very effective generation centre and causes a dramatic increase of the leakage current.

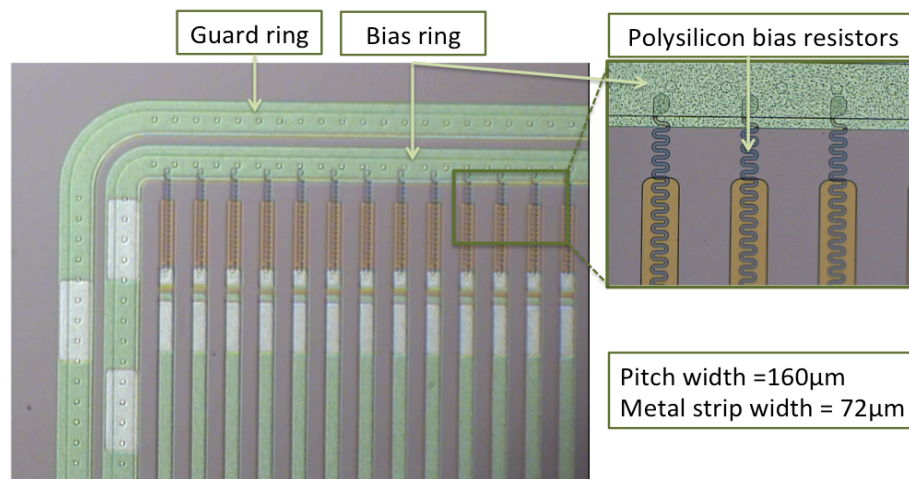


Figure 2.6.- EASY sensor view showing the guard ring, the bias ring and polysilicon resistors.

These features can be observed in the photograph of the silicon micro-strip detector, which is represented in Figure 2.6.

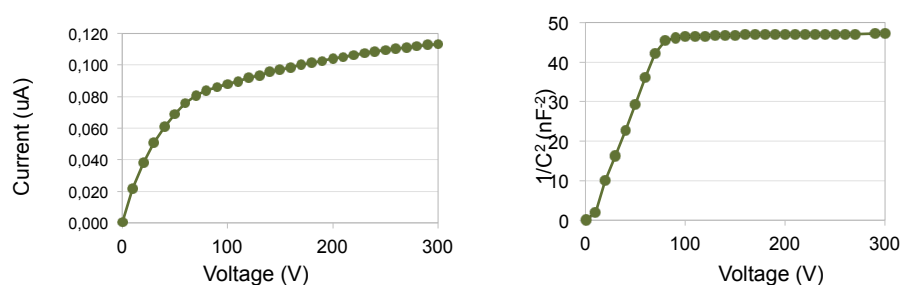


Figure 2.7.- Typical CV and IV curves of the EASY sensors before assembly.

For the EASy sensors, leakage current and capacitance measurements are done before they are assembled un the Sensor Unit. The measurements of a typical sensor are shown in Figure 2.7.. By plotting $1/C^2$ the depletion voltage can be determined, the typical value of depletion voltage for these sensors is between 60-80V, i.e. above those

values the capacitance is constant.

2.4 SIGNAL FORMATION

A minimum ionising particle (*MIP*) that traverses a silicon detector loses energy mainly by ionization (*Bichsel*). When the ionising particle passes through a silicon atom in the lattice, this will tend to liberate a loosely bound valence electron generating an electron-hole pair. The electron will be ionised at an excited energy state and via collision will enter thermal equilibrium with the lattice as a free electron in the conduction band. Occasionally the ionising particle will interact with a more tightly bound electron than the silicon valence electrons and, as a result, will create an electron with a significant amount of kinetic energy. This liberated electron can cause secondary ionisation of the silicon. The energy deposited for this interaction is therefore higher than that for the interaction with the valence electrons. As a result of these rare high-energy events the energy spectrum of the deposited energy in the silicon detector is a non-symmetric distribution as shown in Figure 2.8.a. This distribution was first described by Landau and therefore it takes his name. The Landau theory assumes a free charge electron cross section neglecting the atomic bonds. So, a Gaussian distribution convoluted with a Landau curve is used to reproduce the experimental energy distribution as shown in Figure 2.8.b.

Due to the non-symmetric nature of the distribution the mean value is higher than the most probable value. For a *MIP* the mean energy loss per unit length is 3.88 MeV cm^{-1} or 116 keV for $300 \mu\text{m}$ of silicon; whereas the most probable energy loss is approximately 0.7 times this or 81 keV for a $300 \mu\text{m}$ thick detector. An average energy of 3.6 eV is required to produce a single electron-hole pair in silicon. This results in a mean signal from a $300 \mu\text{m}$ thick detector of 32000 electrons or a most probable value of around 23000 electrons; which is equal to 3.6 fC . It is the most probable energy that is used for calculations of collected charge from a silicon detector.

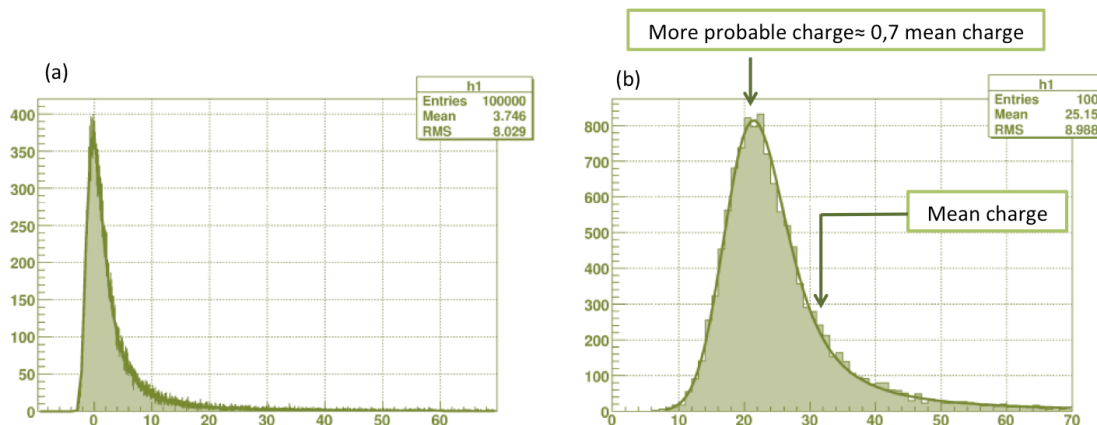


Figure 2.8.- Examples of a (a) Landau distribution, and a (b) Landau convoluted with a Gaussian distribution.

2.5 SPATIAL RESOLUTION

The signal pulse at the strips is amplified and integrated by the readout chip to measure the total charge deposited into the micro-strip detector. Since all the strips are

read out, the strip to which the signal arrives gives information about one coordinate of position of the traversing particle. So, a micro-strip detector is a sensitive position system and can be used as a tracker.

The position resolution of a silicon detector is determined, to a first approximation, by geometrical factors, as the width of the electrodes and the pitch. In practice, it is the size of the readout electronics that imposes constraints on the size of the detecting device. The broadening of the charge distribution can be used to improve the intrinsic resolution of the detector, as the charge is shared between more readout electrodes. In a detector characterised by a strip pitch larger than the diffusion width, the differences between the measured and the actual positions have a Gaussian distribution with a standard deviation:

$$\sigma^2 = \frac{p^2}{12} \quad (11)$$

therefore the resolution is the strip pitch divided by $\sqrt{12}$. For our sensor strip of 160 μm pitch, the σ corresponds to 52 μm . The centre of gravity of the resulting signal can be calculated, increasing the accuracy of the measurement compared to the case where just the information of the electrode collecting the charge is used.

2.6 SOURCES OF NOISE

The signal generated in silicon detectors is generally of small amplitude (around 24000 electrons), hence amplification and shaping stages are required for its further processing. A charge sensitive preamplifier is typically used, avoiding any dependence on the detector capacitance change with temperature. Inevitably, noise will be introduced by the readout electronics affecting the charge measurement. The total noise of the system is measured as an equivalent noise charge at the input of the amplifier. The input charge that produces a signal amplitude equal to the *rms* noise), ENC , at the output is given by:

$$ENC_{TOT}^2 = ENC_{PA}^2 + ENC_I^2 + ENC_{RP}^2 + ENC_{RS}^2 \quad (12)$$

where ENC_{PA} is the preamplifier noise given by:

$$ENC_{PA} = A + B \times C_{load} \quad (13)$$

A and B are pre-amplifier constants and C_{load} is the capacitive load at the input of the pre-amplifier. ENC_I is due to the detector leakage current (I) for CR-RC shaper and it has the expression:

$$ENC_I = \frac{e}{q} \sqrt{\frac{qI\tau}{4}} \quad (14)$$

τ is the shaping time of the shaper. ENC_{RP} is the thermal noise from the parallel resistor:

$$ENC_{RP} = \frac{e}{q} \sqrt{\frac{\tau KT}{2R_b}} \quad (15)$$

R_b is the bias resistor of the detector. Finally, ENC_{RS} is the noise from the serial in the circuit,

$$ENC_{RS} = 0,395 \times C_{load} \sqrt{\frac{R_S}{\tau}} \quad (16)$$

where R_S is the resistance of the readout chip. The two main noise sources, which contribute in silicon detectors, are the **detector capacitances** and the **leakage currents**.

2.7 TRIGGER MODES.

A trigger system determines when a particle arrives to the detector and activates the data acquisition defining an event. The EASY system implements two trigger modes: Diode Trigger and Self-Trigger.

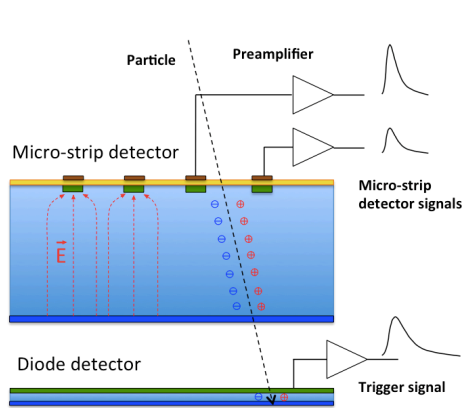


Figure 2.9.- Sketch of the EASY diode trigger.

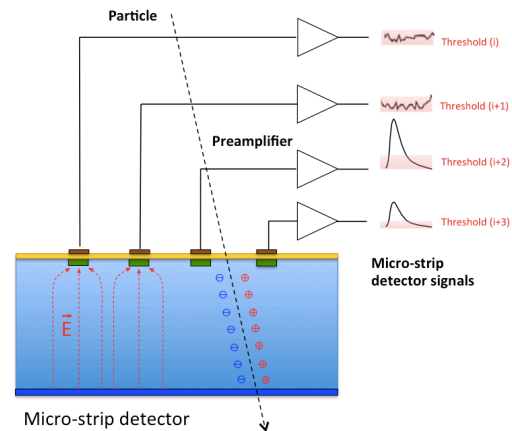


Figure 2.10.- Sketch of the EASY self-trigger.

The Diode Trigger, sketched in Figure 2.9, consists of discriminating a signal generated by a low noise silicon diode. The silicon diode is mounted underneath the micro-strip sensor with a gap of few millimetres. When a particle crosses the micro-strip and reaches the diode, the generated charge in the diode is discriminated to produce the trigger signal that starts the acquisition. The Diode Trigger mode is suitable for minimum ionising particles (*MIPs*) when studying the passage of particles through matter.

The Self-Trigger signal is generated by the fast comparator built in the BEETLE chip when an incident particle hits the micro-strip sensor. Each one of the 128 comparators has a different offset and response. Thus, an individual calibration of each comparator is needed in order to calculate the individual threshold value for each channel. With this calibration the same sensitivity for all channels is obtained. The EASY software provides an automated procedure to generate and calibrate all the thresholds. Figure 2.10 shows a sketch of the Self-Trigger. The Self-Trigger mode is convenient for acquiring data when the incident particles are completely absorbed, as it can be the case of photons or alpha particles.

i

3 DATA ACQUISITION PROGRAM.

3.1 DOWNLOADING ALIBAVA-GUI.

Alibava-gui is a graphical user interface, written in C++, that controls the Control Unit of the EASY system. It is able to configure the device, receive the data via USB bus and store it in a file for further analysis. Alibava-gui also monitors the data while in acquisition mode. Alibava-gui can be run in Windows, Linux and MacOS. The Alibava-gui data acquisition program can be downloaded from the web page:

<http://www.alibavasystems.com/>

going to DOWNLOADS -> EASY. The instructions for installation can be found in the same web.

3.2 STARTING ALIBAVA-GUI.

Once the installation is completed, the EASY icon will be display to run the program. The application can also be aunched by typing:

alibava-gui [options] [config_file]

where *config_file* is a file where all the settings have been saved and the *options* are shown in Table 3.1. In general, *Alibava-gui* runs in Graphic User Interface (GUI) mode, therefore all the options listed below can be set in the various dialogs as describe in next sections. However, one could give some of the options at the start of Alibava-gui to have those values by default to begin the data acquisition.

There are 5 run types:

- **Calibration:** Alibava-gui programs the BEETLE chips to inject calibration pulses to all the channels in order to characterize the electrical behaviour of the ASIC. The calibration also allows obtaining the gain of the ASIC.

- **Laser synchronization:** Alibava-gui sends a pulse that can be used to trigger the laser. This run mode scans the delay between the pulse sent by the Control Unit to the laser and the acquisition. That delay will be later used when measuring so that the system samples at the maximum of the signal produced by the laser.
- **Pedestals Run:** Alibava-gui generates an internal trigger that will allow computing the baseline for pedestals and its variation (i.e. the noise).
- **Laser Run** makes a run where a laser beam injects the charge; one needs to run the laser synchronization mode beforehand in order to read back the optimal signal produced by the laser.
- **RS Run** (Radioactive Source Run) makes a run in which the acquisition is triggered by signals above the threshold in the input connectors suitable for radioactive source or cosmic data.

When starting Alibava-gui the main window displayed in Figure 3.1 appears. The run types are selected on the right side of the window (Figure 3.1.a). The right buttons next to each run type open a dialog window to configure the run parameters. All the settings can be stored in a configuration file by clicking *Save* in the *File menu* (use the extension *.ini* for the configuration file). Configuration files can be load by clicking on

Table 3.1- Alibava-gui options.

--gui	Shows the main GUI. This is the default.
--no-gui	The program runs without a GUI.
--emulator	Simulates (Emulates) the data with no system connected. Useful to get familiar with the application.
--nevts=n	Sets n as the maximum number of events in the run.
--sample=n	Number of events to acquire in the motherboard before transmitting the data to the PC.
--dev=/dev/ttyUSBn	Sets /dev/ttyUSBn as the port to communicate with the motherboard in case n is not the usual 0.
--out=out_file_name	Sets the path and name of the output data file.
--pedestal	Acquires a Pedestal run in no-gui mode.
--source	Acquires a Radioactive Source run in non-gui mode. Other required settings should be provided through a configuration file.
--calib	Acquires a Calibration run in non-gui mode. Other required settings should be provided through a configuration file.
--laser	Acquires a Laser run when in non-gui mode. Other required settings should be provided through a configuration file.
--activate-plugin	Activates the plugin if defined in the configuration file.
--firmware=n	Forces a given version of the firmware.
--soap-port=nn	Port number of the Alibava-gui soap server

Open in the *File menu*. There are more configuration settings that can be set by clicking on the different items of the Settings menu described in section 3.4.

The DAQ buttons (Figure 3.1.b) *Starts* and *Stops* initiate or end the acquisition. One can monitor the number of acquired events, the elapsed time, the acquisition rate and the efficiency during the data acquisition (Figure 3.1.b). The acquisition rate is integrated in 1-second time windows, so 0 values while the data is being read out from the USB port are expected. The efficiency is the number of events that pass the criteria defined in the Analysis dialog window described in section 3.1.3.

There is a collection of tabs (Figure 3.1.c) to allow monitoring the data during acquisition: *Signal*, *Pedestal*, *HitMap*, *Temperature*, *Time* and *Noise/Common mode*. On some of the tabs, there are buttons that will refine the information displayed on the histograms.

The *LogData* button opens a dialog window to save the data in a file, notice that **data should be saved before starting the run**.

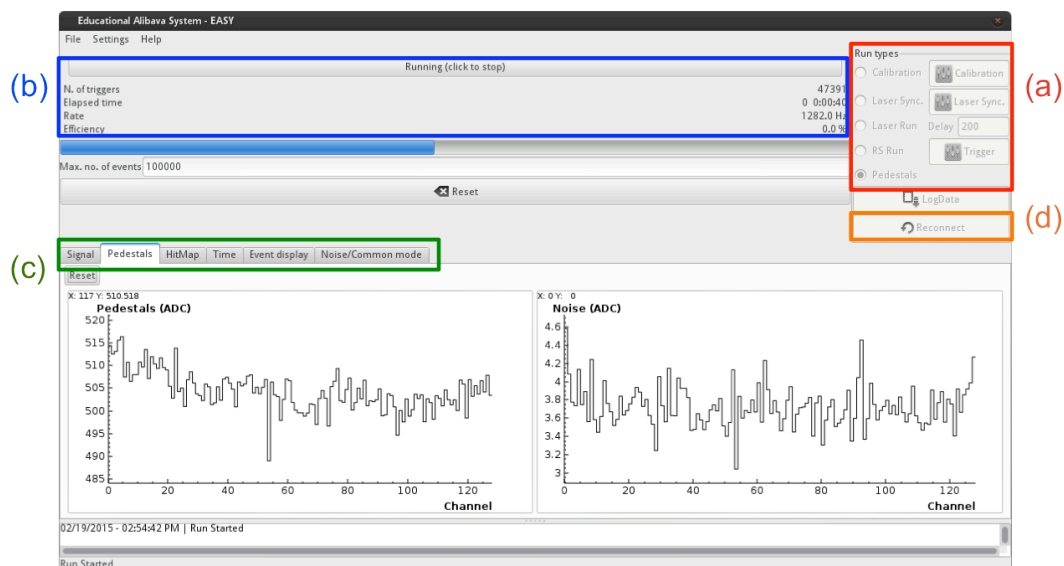


Figure 3.1- Main screen of Alibava-gui during a Pedestal run.

Finally, the *Reconnect* button (Figure 3.1.d) helps you to connect the system back in case it is accidentally disconnected. Note that the manual reset button at the rear of the Control Unit can also be used if needed. If the EASY system is unplugged from the USB without quitting *Alibava-gui* it should be reset before operating with it again.

3.3 TAKING DATA

To take data, select the run type, set the specific parameter when needed and click on the DAQ button (*Start* in Figure 3.1). To store the data for further analysis, press the *LogData* button and define the data file to save the data, before starting the run. A dialog window will pop up where you can enter the name of the output file. So, when clicking *Start*, the run will start and the data will be recorded into the data file.

The following sections describe the different run types.

3.3.1 CALIBRATION RUN

The system injects pulses in the readout ASIC (BEETLE) for calibration. An Analogic Digital Converter (ADC) reads the pulses in arbitrary ADC counts. From the calibration curve one can obtain the conversion of ADC counts to charge (number of electrons). This will be useful in other modes to know the collected energy.

The calibration run is done in two steps:

- strobe delay scan,
- charge scan of the test pulse.

The strobe delay scan sets the delay between the injected signal that generates the calibration pulse, and the clock rising edge of the BEETLE 128th slots of the pipeline. The time of the pulse maximum defines the delay; this is, the time where the charge will be sampled for the calibration.

Before starting the delay calibration run the proper parameters must be set. By pressing the *Calibration* button shown in Figure 3.1.a the calibration window of Figure 3.2 pops up to allow setting the run parameters.

To perform a strobe delay scan we have to select *Delay* in the window of Figure 3.2, by default the delay is set to 85 ns and the pulse injected to 30720 electrons (around 5fC).

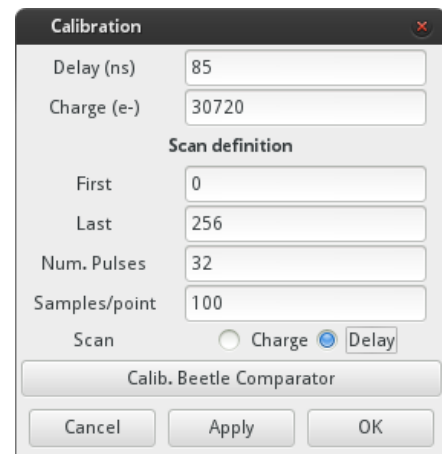


Figure 3.2- Settings for the Delay calibration scan.

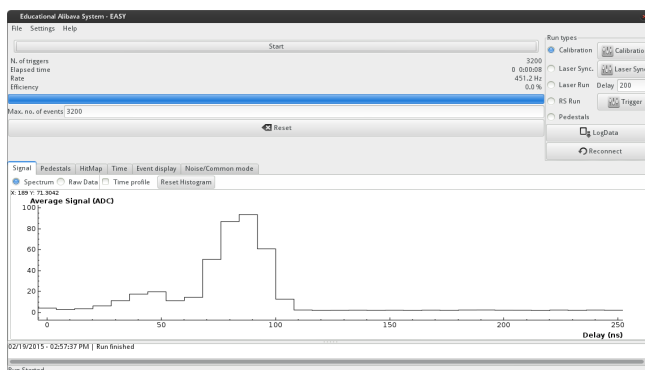


Figure 3.3 - Display of the pulse shape injected for calibration, the maximum of the pulse will define the in strobe delay.

Figure 3.2 shows the setting for the delay scan after selecting *Delay*. The *First* and *Last* options of the settings define the time interval to reconstruct the pulse, *Num. Pulses* are the number of input pulses in the interval of delay time and *Sample/pulse* are the number of samples per pulse that will be acquired. After saving the setting, by pressing *Apply* and *OK*, the strobe delay scan can be started. To start the calibration run, first, *Calibration* has to be selected in the main window (Figure 3.1.a) and after *Start* can be pressed (Figure 3.1.b). The reconstructed pulse

can be displayed during the data acquisition by activating the *Signal* tab (Figure 3.1.c) Figure 3.3 shows the reconstructed pulse as displayed in the main window. The maximum of the pulse is reached at 85ns for this particular case, but it will change with the BEETLE parameters. This value should be entered as default for the strobe delay parameter (Figure 3.2).

In the charge scan the system injects pulses with different amplitudes to get the gain and offset of the characteristic curve of the preamplifier in all the ASIC channels. Note, as mentioned before, to find the correct gain value one has to set first the strobe delay to sample the signal where it reaches the maximum value.

To set up the parameters to perform the charge scan, access the calibration parameter window (as done in the strobe delay scan) and activate *Charge* (Figures 3.4). The parameters *First* and *Last* define the interval of injected charge in electrons, whereas *Num. Pulses* is the

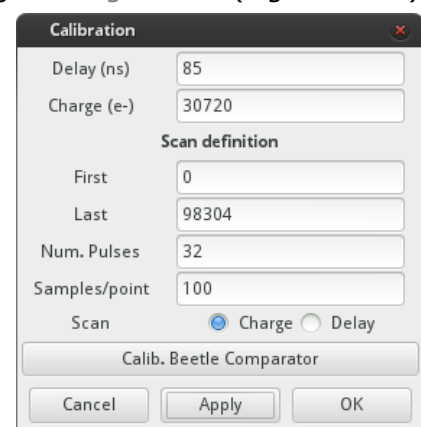


Figure 3. 4- Setting for the Charge calibration scan.

number of input pulses in the interval of charge and *Sample/pulse* is the number of samples per pulse that will be acquired for each calibration pulse. After saving the run parameters, the charge calibration run start by clicking *Start*.

Figure 3.5 shows the calibration curve, i.e. reconstructed charge in ADCs units as a function of the injected charge in electrons. For this particular run the maximum injected charge injected was 98.304 electrons (the maximum charge range of the BEETLE is 110.000 electrons). During the calibration run, the *Event display* tab can be activated to control the charge injection in each channel. The calibration curve corresponds to a particular channel (channel 60 by default), to display the calibration curve of another channel see section 3.4.2.

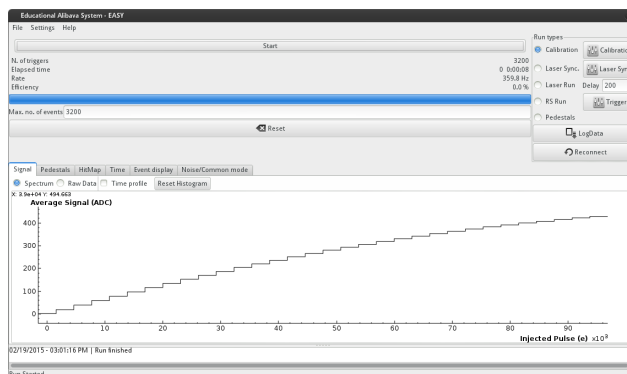


Figure 3.5- Charge calibration scan to get gain and offset.

The data of the histograms can be loaded to a file by clicking the mouse right button over the histogram.

Notice that during calibration, the BEETLE **Latency has to be set to 128** to have the pulse in the time window for calibration.

Since the calibration depends on the BEETLE parameters, be sure you are getting your calibration curve with the same settings as your analysis data (laser or radioactive source data), with the exception of the Latency that has to be set to 128 during calibration and set to your working value during data acquisition.

3.3.2 LASER SYNCHRONIZATION

The Control Unit is able to send a pulse that is used to trigger the laser system. Prior to conducting a laser run, the system has to be synchronized. The Laser synchronization scans the delay between the pulse sent by the Control Unit and the acquisition so that the system can sample at the maximum of the signal produced by the laser. By clicking on the button *Laser Sync.* on the main window (Figure 3.1.a) a dialog box like the one in Figure 3.6 will pop-up to set the parameters of the delay scan.

The parameters *From*, *To* and *Step* define the time interval that will be scanned and the time step to increase the laser delay. The *Sample/point* specifies the number of events that will be acquired for each value of the laser delay.

After setting the parameters for the Laser scan synchronization, the run will start by selecting *Laser Syncr* on the run type menu (Figure 3.1.a) and pressing the button *Start* (Figure 3.1.c). By selecting the *Signal* tab on the main window the display of Figure 3.7 will be shown. The maximum of the signal distribution is used to set the Laser delay (Figure 3.7a). In the example of Figure 3.7 the laser delay is 118ns.

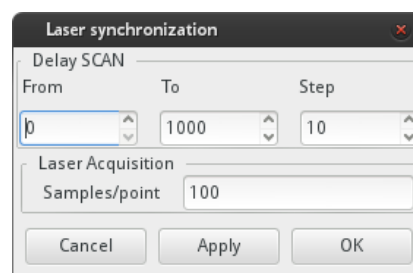


Figure 3.6 - Laser Synchronization scan parameters.

3.3.3 PEDESTAL RUN.

Pedestals are recorded when reading the output pulse with no signal injected and establish the offset of each channel. Electronic noise of each channel (as described in Section 2.6) is defined as the RMS of the pedestal. Pedestal and noise determination is mandatory previous to any determination of charge deposition in the sensor. The pedestal run is also useful to verify if the system performs properly, therefore a pedestal run should be done to start any session of data acquisition.

Alibava-gui can compute pedestals on-line either by making a dedicated pedestal run or estimating the pedestal and noise while taking data.

To performance a dedicated pedestal run, select the *Pedestals* in the main window (Figure 3.1.a) and start the run by pressing *Start* (Figure 3.1.b). When selecting the tab *Pedestal* in the main window, histograms as the ones in Figure 3.1 are obtained. The pedestals and noise can also be used for a posterior data analysis; therefore the measured pedestals can be saved in a file via the *Save Pedestals* item in the *Settings menu*.

The format of that pedestals file is:

- each line corresponds to one channel with line zero for channel 0
- each line contains the pedestal value, followed by a white space-like character (space or tab) and then the noise value

An alternative is to save the pedestal and noise by right-clicking on the histogram as explained in section 3.6, then the pedestals and noise will be saved in two independent text files.

Pedestals and noise are also estimated during the data acquisition and can be saved at the end of the run. Note that for some type of runs, pedestals calculation is not needed. This is the case of the calibration; laser synchronization and laser run since, a priori, the channels will always have fix amplitude.

3.3.4 LASER RUN

In a Laser Run the charge is injected in the sensor by a pulsed laser located in the Control Unit. The charge injected is constant and can be oriented to a fix position in the sensor by using the horizontal micrometre screws of the laser positioning system on the Sensor Unit. The vertical micrometre screw allows focusing the laser signal. Before starting a laser run the system needs to be synchronised as described in section 3.3.2 and the correct delay set in the main window. To start the run, select *Laser Run* in the main window (figure 3.1.a) and press Start (Figure 3.1.c).

3.3.5 RADIOACTIVE SOURCE RUN (RS)

The Radioactive Source (RS) mode allows data acquisition from a radioactive source or from cosmic rays. RS mode needs specific triggers and parameter settings

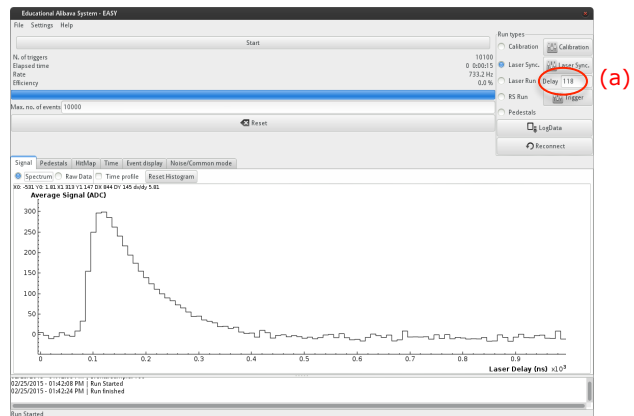


Figure 3.7.- Laser Synchronization signal display.

before starting the acquisition; those settings are described in section 3.4. To start the run, select *RS Run* in the main window (figure 3.1.a) and press Start (Figure 3.1.c).

3.4 CONFIGURING EASY

EASY is a very flexible system that allows the use of different acquisition modes, use several trigger signals, perform some level of data analysis, modify the ASICs parameters, define the data format, etc. In this section the way to configure the data acquisition is described.

There are a number of ways in which you can configure *Alibava-gui*. Once this is done, one can always save that particular configuration to be restored and used in the future. To save the current configuration click on the *Save* or *Save As* items on the *File menu* of the main window. Saved configurations can be loaded afterwards either by giving the configuration file path when starting *Alibava-gui* or by choosing a configuration file through the *Open* item in the *File menu*.

Most of the configuration parameters can be accessed through the *Settings* or *Preference* menu as shown in Figure 3.8. Each of these menu items will allow configuring different aspects of the *Alibava-gui* behaviour and are described in the next subsections.

Settings:

Data File Format	Ctrl+F
DAQ	Ctrl+D
Beetle	Ctrl+B
Trigger	Ctrl+T
Comparator	Ctrl+C
Analysis	Ctrl+A
Latency	Ctrl+Y
Load Pedestals	Ctrl+R
Save Pedestals	Ctrl+P

Figure 3.8. - Settings accessible through the Settings item in the main window menu bar.

3.4.1 DATA FILE FORMAT

Data File Format allows selecting between HDF5 format and Binary format. The default format is HDF5 (*The HDF group*), which can easily be read from Python, Matlab or Octave. Section 3.8 describes the format of the data.

3.4.2 DAQ CONFIGURATION

The *DAQ configuration* defines how to perform the data acquisition and allows modifying the following parameters:

- *Calibration monitor channel*: this is the channel whose characteristic curve will be shown in the monitor window (Figure 3.5) while running a pulse calibration.
- *Sample size*: this is the number of events stored in the Control Unit memory before sending them to the PC. This is only used in Pedestals, Laser and RS modes.
- *Number of events*: maximum number of events. When the number of events acquired equals this value the run stops.
- *Delay*: maximum time without data before

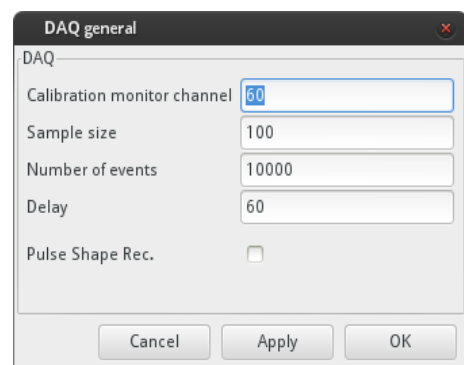


Figure 3.9. - DAQ configuration window.

Alibava-gui realizes that there is a communication problem and stops the acquisition.

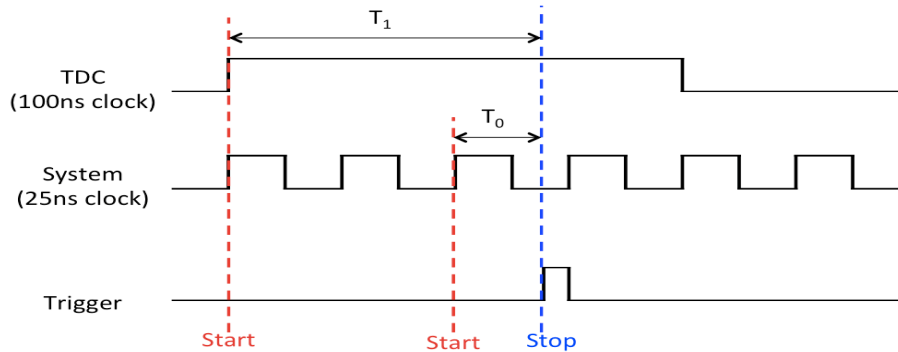


Figure 3.10.- Time scheme of the TDC system time associate to the measured charge .

- Pulse Shape Rec.:** When running in Radioactive Source mode, the pulse shape can reconstructed. For that, the system has an internal Time Digital Converter (TDC) with a range of 100ns and a system clock with a period of 25ns, as sketched in Figure 3.10. The raising of the signal defines the start of timing, if a Trigger signal arrives within the 100ns of the TDC pulse, that trigger defines the end of the time counting, then the time measured is T_1 . If the *Pulse Shape Rec* is selected in the DAQ configuration menu T_1 is associated to the charge measured by the system for this trigger. This allows measuring times as large as the full TDC range (100ns). The full pulse shape is reconstructed by plotting the average of the signal as a function of the TDC measured (T_1). If *Pulse Shape Rec* is not selected the time associated to the charge recorded is T_0 , this is the time between the raising edge of the internal clock and the trigger signal. In this case the pulse cannot be reconstructed but the data acquisition is faster.

3.4.3 BEETLE CONFIGURATION

The BEETLE ASIC is an analog readout chip that was originally designed for the LHCb tracking detector (Löchner and Schmelling, M). The chip has 128 channels with an amplifier and a shaper. A 40MHz clock (LHC bunch-crossing frequency) samples the amplified and shaped signal pulse. This value enters an analog pipeline; consequently each readout window is 25nd long. As the pipeline has a finite number of elements, when the new readout value enters the pipeline, the information of the oldest is lost. When the Control Unit send an external readout trigger to the ASIC, the information of the oldest readout is transferred off the chip to the Control Unit.

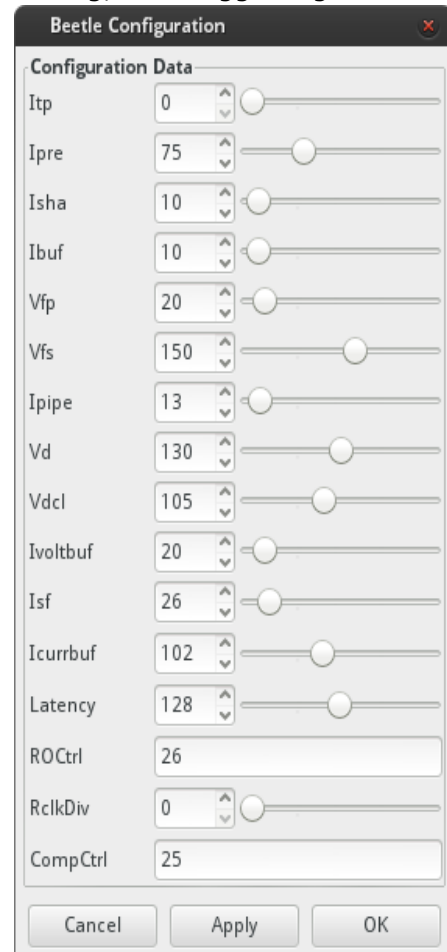


Figure 3.11.- BEETLE configuration with the parameter.

There is a large variety of parameters to configure the ASIC and to define the pulse shape. The BEETLE parameters are set by clicking on the *Beetle* item of the *Settings menu* as shown in Figure 3.11. A full description of the BEETLE setting could be found in reference (Löchner and Schmelling, M).

The most relevant parameters for the EASY are V_{fp} , V_{fs} and the latency. V_{fp} defines the time constant for discharging the preamplifier's integration capacitor and therefore the tolerable input charge rate. V_{fs} is the shaper feedback voltage; increasing V_{fs} will enlarge the peaking time. Latency is the trigger latency with 160 sample intervals of 25ns. The BEETLE latency can also be set using *Latency* item on the *Settings menu*. The values of V_{fp} and V_{fs} have to be set to make the pulse larger enough to ensure we will easily sample on its maximum in the 25ns readout window. With the latency parameter the pulse sampling can be moved in 25ns steps to synchronise our trigger with the readout window. Increasing the latency in one unit will make the pulse arrive 25ns later.

To set up the optimum BEETLE parameters one can study the pulse shape using the strobe delay calibration described in section 3.3.1. The pulse of Figure 3.3 corresponds to $V_{fp}=0$, $V_{fs}=0$ and Latency=128, the standard parameters for data acquisition in LHC. The data from the histogram can be saved in a file for further analysis. The optimum parameter should make the pulse large enough to have flat amplitude over the 25ns window for the correct charge sampling.

Figure 3.12.a shows the pulse shape variation with V_{fs} ; by increasing V_{fs} the rising time increase and also the pulse becomes larger. The optimum value is 150. Once V_{fs} is fixed to 150, V_{fp} contributes to enlarge the pulse, the optimum values go from 5 to 20 (Figure 3.12.b). Finally, the latency moves the pulse in 25ns steps (Figure 3.12.c) and the optimum value for the latency depends mainly on the trigger mode.

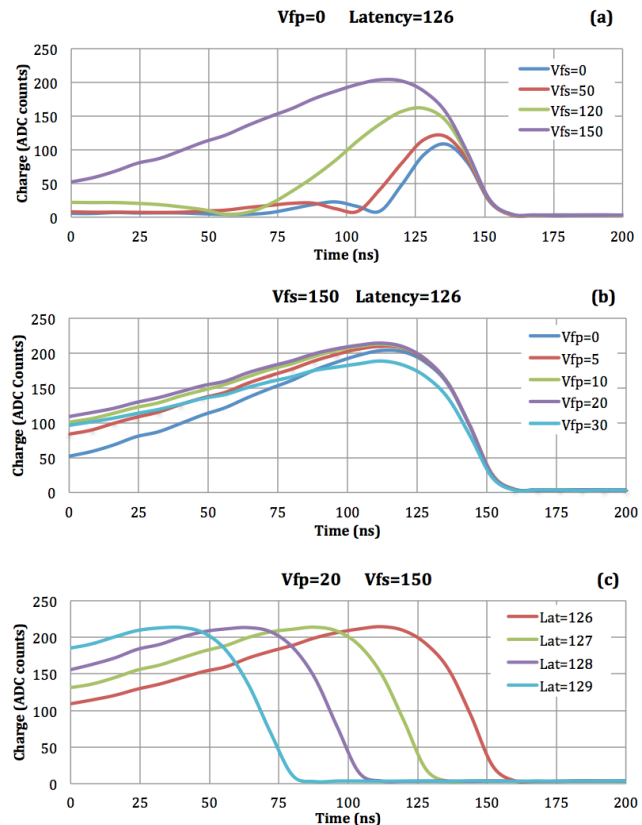


Figure 3.12.- Different pulse shapes reconstructed with the strobe delay calibration using different depending BEETLE setting. (a) Pulse shape variation with V_{fs} with $V_{fp}=0$ and Latency=126. (b) Pulse shape variation with V_{fp} with $V_{fs}=150$ and Latency=126. (c) Pulse shape variation with Latency V_{fp} with $V_{fs}=150$ and $V_{fp}=20$.

3.4.4 EXTERNAL TRIGGER CONFIGURATION

To read the charge deposition from a radioactive source or from cosmic rays an external trigger signal has to be generated. There are two types of external trigger: *Trigger In* and *Trigger Pulse in*. The external trigger can be configured by clicking the *Trigger* item in the *Settings menu* or by clicking the *Trigger* button in the main window (Figure 3.1.a). In both cases the dialog shown in Figure 3.13 will pop up. The characteristics and parameters of the external triggers are:

- *Trigger In* uses two external signals to produce the trigger, for instance, from two photomultipliers. The input signals are supposed to be negative, as well as the corresponding thresholds. The trigger will be fired either by both signals (*AND*) or any of the two (*OR*) are below the threshold programmed. To use this trigger, select *Trigger In*, *AND* or *OR* and the thresholds for each trigger signal (*Thrs. Trigger In 1* and *Thrs. Trigger In 2*). Units are in mV.
- *Trigger Pulse in* uses one single trigger signal, for instance from the diode placed below the detector (*diode trigger*) or from the signal of the energy deposition in the detector (*Self-trigger*). In this case, there are two thresholds, one positive and one negative. The Control Unit will produce a trigger for any signal which is either above both values (a positive signal) or below both thresholds (negative). If the input pulse falls between the two values it will not produce a trigger. To use this trigger, select *Trigger Pulse In* and set the positive (*Thrs+ Trigger Pulse In*) and negative thresholds (*Thrs- Trigger Pulse In*). Units are in mV.

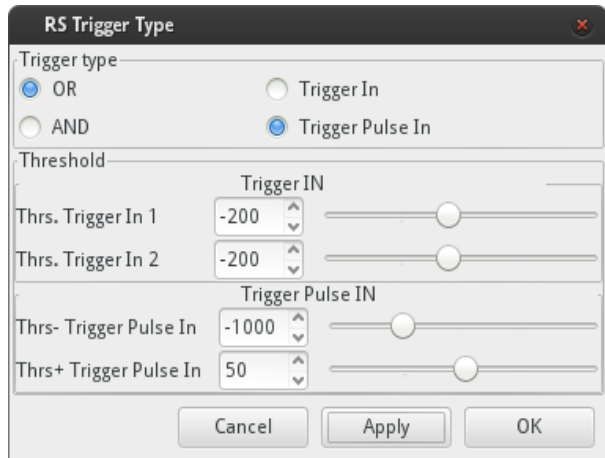


Figure 3.13.- Trigger configuration.

3.4.5 BEETLE COMPARATOR CONFIGURATION

The behaviour of the BEETLE comparator can also be configured as shown in Figure 3.14. This is only useful in the Self-Trigger mode. The upper button is used to enable and disable this feature. Then, one sets the appropriate parameters such as the polarity, trigger mode, threshold, some advance parameters and, also, the channel mask and threshold corrections of the individual channels. The BEETLE chip documentation provides more information about all these parameters. The most important feature of this application is the capability of masking unwanted channels.

3.4.6 ANALYSIS CONFIGURATION

The data is monitored during the acquisition and several histograms can be displayed. The user can decide between displays of the raw data or the reconstructed charge spectrum. To reconstruct the charge spectrum, the user can set different parameters to control the data processing and the data analysis. The charge spectrum is

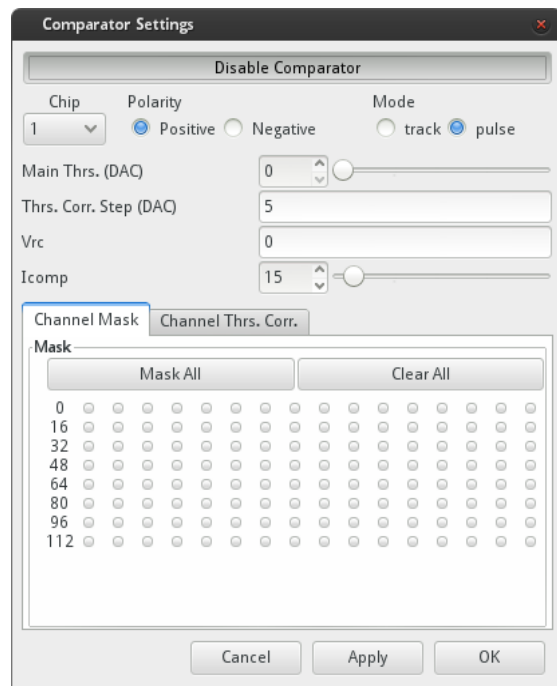
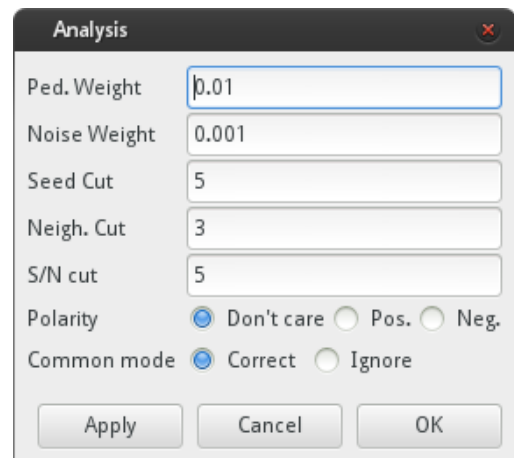


Figure 3.14.- BEETLE comparator configuration.

calculated using the channel with a given signal over noise value and grouping the channel in clusters to estimate the total charge deposition in the detector of the particles under study. Figure 3.15 shows the parameters to configure the analysis. *Alibava-giu* estimates the pedestals and noise during data acquisitions. Parameters *Ped. Weight* and *Noise Weight* control the estimation of those parameters. *Seed Cut* and *Neigh. Cut* are used to define cluster seed number of neighbour channels to consider. *S/N cut* define the *channel* to consider in the cluster (those channels with a signals over noise larger than *S/N cut* parameter). For the analysis one can select to use only positive pulses (*Pos.*), only negative pulses (*Neg.*) or both (*Don't care*). The common noise can also be subtracted (*Correct*) or not (*Ignore*).



The 'Analysis' dialog box contains the following fields and options:

- Ped. Weight:** 0.01
- Noise Weight:** 0.001
- Seed Cut:** 5
- Neigh. Cut:** 3
- S/N cut:** 5
- Polarity:** ☒ Don't care, ☐ Pos., ☐ Neg.
- Common mode:** ☒ Correct, ☐ Ignore
- Buttons:** Apply, Cancel, OK

Figure 3.15.- Analysis configuration.

3.4.7 LATENCY.

The latency window gives direct access to modify the BEETLE latency since this parameter has to be changed several times during the exercises.

3.4.8 LOAD AND SAVE PEDESTALS

Pedestals and noise can be saved after a pedestal run or a radioactive source run in a text file. This pedestal file can be loaded at any time to be used to process the data during the data acquisition. Notice that for large statistics the pedestals and noise estimations during data acquisition are completely consistent with those obtained in a pedestal run.

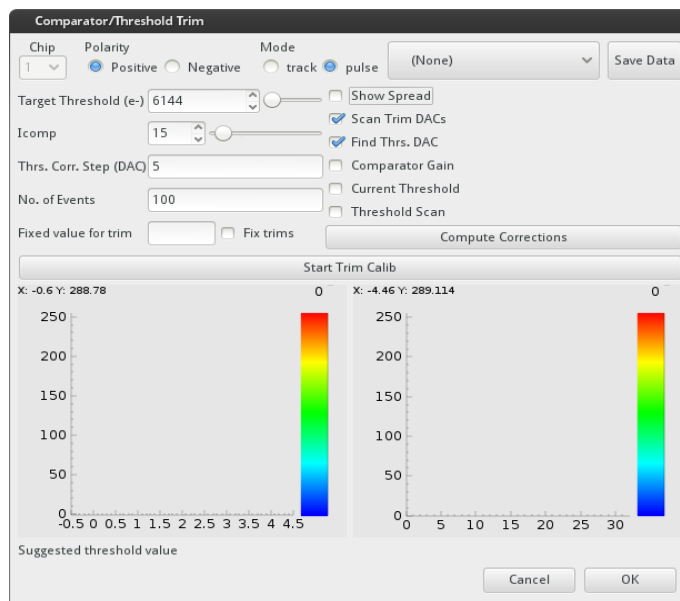


Figure 3.16.- Calibration of the Threshold correction for the channels.

3.5 CALIBRATION OF THE INDIVIDUAL CHANNEL CORRECTIONS TO THE COMPARATOR THRESHOLD

The comparators on the BEETLE chip have a no negligible spread and therefore the chip provides mechanisms to align thresholds of all the channels for a given working global threshold. This is a quite large procedure but *Alibava-giu* provides an automatic way to do it.

The procedure is based on counting the number of triggers for a given configuration of the threshold and the channel corrections. This

usually produces the so-called *s-curves* which, when properly normalized, yield a:

- 1 when all the events produce a trigger,
- 0.5 when the threshold is equivalent to the mean of the input charge distribution
- 0 when no event produces a trigger.

This is done with the BEETLE calibration circuit. This system produces alternate polarities for each channel, always with the same absolute value of the input charge. So, when the user programs a given number of events, only half of them will have the proper polarity. The two polarizations are taken into account when normalizing so that when the threshold is so low that we trigger on the noise the value of the *s-curve* is 2, instead of 1, since we also trigger in the events with the opposite polarity. This defines a characteristic

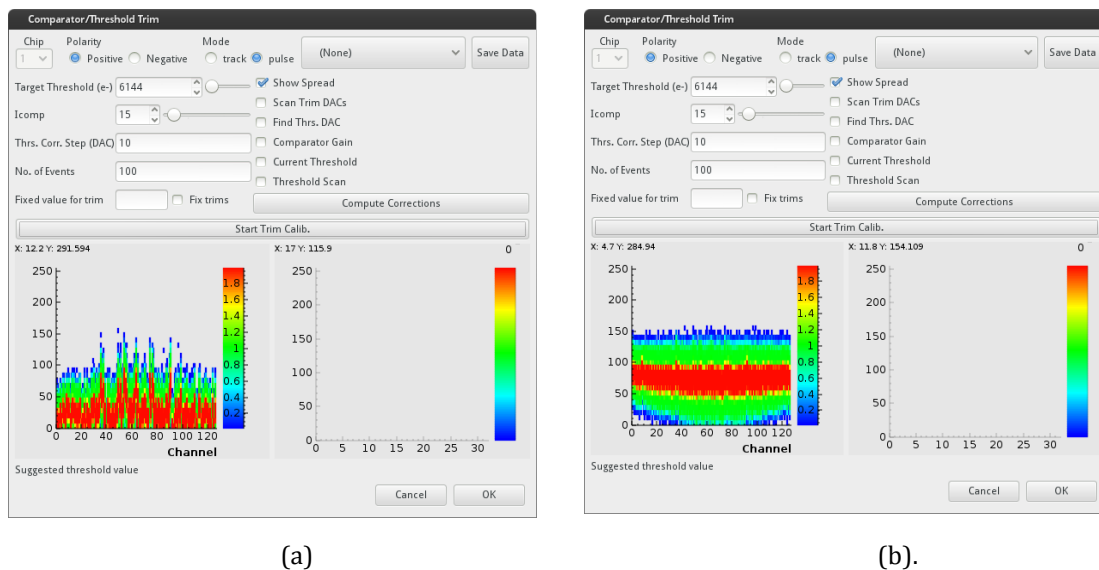


Figure 3.17.- Channel comparator spread before (a) and after alignment (b).

red band in the histograms produced. There is another "effect" that related to the case in which we trigger also on the undershoot of the pulse in the events with the opposite polarity. This explains why the *s-curves* have ending points. Figure 3.16 shows the parameters to set the procedure and to run the comparator threshold scan.

The procedure is as follows:

- Connect the output of the Self-trigger of the Sensor Unit to the *Pulse* input in the Control Unit.
- Configure the trigger (see the section 3.3.4. External Trigger configuration) to trigger on *Trigger Pulse* and set the negative and positive values of the threshold to -500 and 500 respectively.
- Open the Calibration menu and click on the button with *Comparator* (see Figure 3.8). A dialog window as the one shown in Figure 3.15 will pop up.

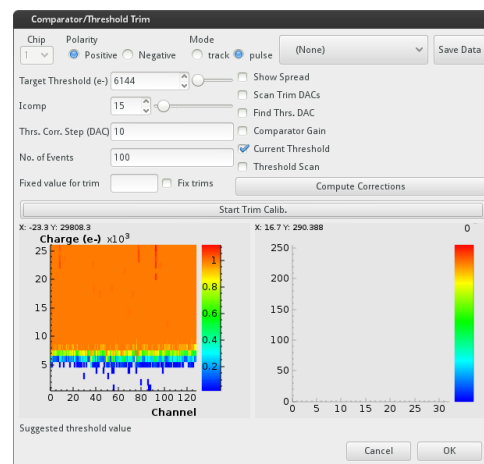


Figure 3.18.- Current setting plot.

- Choose the target threshold (in units of electron charge: 1 fC or 6250 e- are approx. 22.5keV). Select Polarity *Inverting* and Mode *Pulse* and click on the Start button *Start Trim Calib.*
- When the analysis is over, click *OK* if you want to save the settings, or *Cancel* otherwise.
- To save the settings in a configuration file by clicking on the *Save As* item in the File menu.

The right check buttons on Figure 3.16 perform a specific task:

- *Show spread*: This will make a scan of the threshold DAQ values for an input calibration charge equivalent to the desired thresholds. The plot shows if the thresholds are aligned or not, as shown in Figure 3.17.
- *Scan Trim DAQs*: This will make a scan of the threshold correction DAQ for each channel and make a linear fit of the main DAQ resulting as a function of the correction. This will be used to find the final threshold DAQ with the smallest spread among the channels.
- *Find Threshold DAQs*: This has to be done together with the previous scan. It will find the optimal threshold DAQ that minimizes the threshold spread.
- *Comparator Gain*: This will scan the threshold DAQ for different input pulses so that one can see the characteristic curve of each channel's comparator.
- *Current threshold*: This can be used to check what the level of alignment for the current settings is. The plot produced is as shown in Figure 3.18. It makes a charge scan for each channel so that we can see where the threshold is set for each of them. In Figure 3.16 for instance, it is about 6000 electrons.

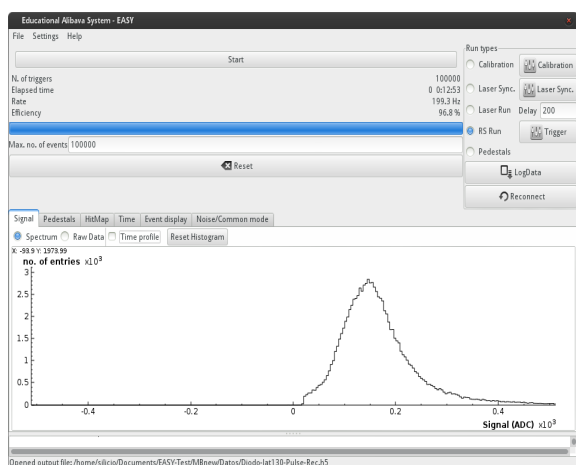


Figure 3.19.- Charge spectrum of a Sr-90 source after data analysis.

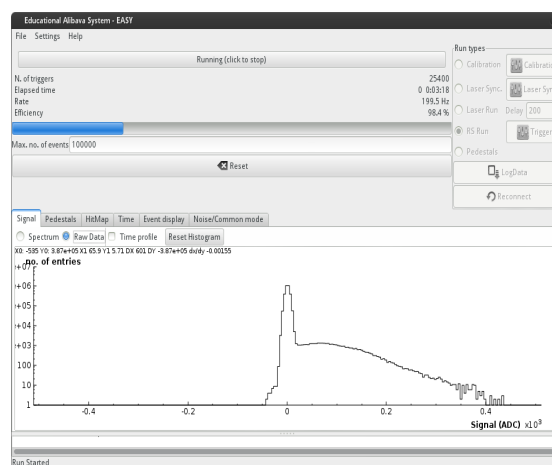


Figure 3.20.- Raw data in logarithmic scale of a Sr-90 source, including all the channels.

3.6 MONITORING THE DATA

There is a set of tabs in the main window (Figure 3.1.c) that show different quantities relevant to the data acquisition. The parameters to monitor depend on the sort of run performed, RS, Laser or Pedestals, as explain below.

3.6.1 SIGNAL TAB

By selecting the *Signal* tab in the main window (Figure 3.1.c) the user can display the charge *Spectrum*, *Raw Data* or the *Time Profile* by selecting the appropriate button. The charge spectrum of a Sr-90 source in ADC units is shown in the display window in Figure 3.19, while the raw data of all the channels in logarithmic scale is displayed in Figure 3.20. To change the attributes of the axes click with the right mouse button over them. Depending on the kind of run the display will be different. For instance, in a Laser run we expect to have constant charge once the laser is properly focused. In a Radioactive Source run a proper Landau distribution is not expected since we plot here the signals sampled all along the pulse. Depending on the parameter set in the analysis configuration menu (section 3.4.6) the distribution of the signal could change depending of the Signal/Noise ratio or the cluster size. By selecting *Time profile* one can display the average value of the signal as a function of the TDC time registered. If *Pulse Shape Rec.* is selected in the DAQ menu (Figure 3.9), the average wave form of the signal pulse in the full TDC range (100ns) will

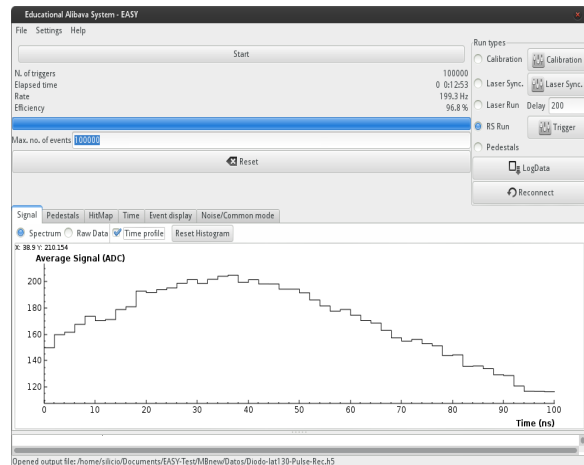
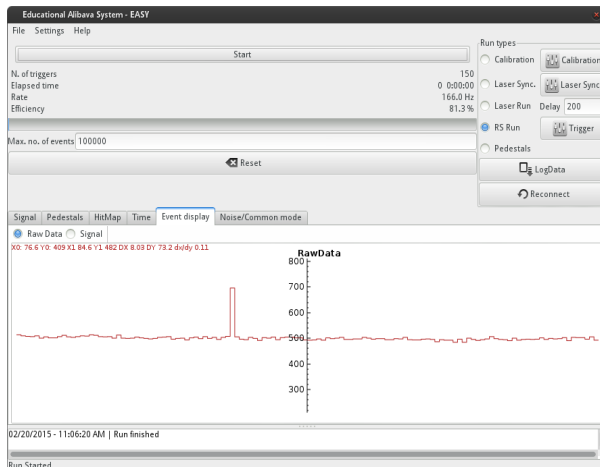
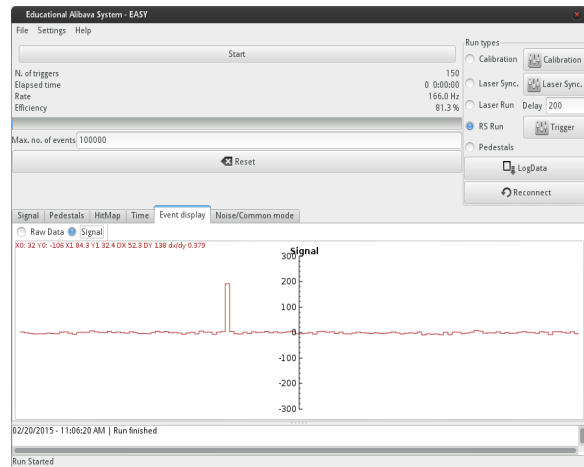


Figure 3.21.- Signal time spectrum (ns).



(a)



(b)

Figure 3.22.- Event Display: raw data (a) and after pedestal and common mode subtraction (b).

be displayed as shown in Figure 3.21 for a Sr-90 source. If *Pulse Shape Rec.* is not selected only the first 25 ns are display and recorded.

By clicking on *Reset histogram* the contents are emptied and the histograms restarted.

3.6.2 EVENT DISPLAY TAB

Figure 3.22 shows the charge collected in each channel for a given event. This

display is obtained by selecting the *Event Display* tab in the main window. One can choose to see the raw data (Figure 3.22.a), without pedestals and common mode corrections or the data after pedestals and common mode subtraction (Figure 3.22.b) by clicking on the proper button on top of the histogram (*Raw Data* or *Signal*). By setting *Sample size* in DAQ menu (Figure 3.9) you can select the frequency of data sampling for the display.

3.6.3 NOISE/Common NOISE TAB

Figure 3.23 shows the average channel noise and the common mode (in ADC units) estimated during the data acquisition event by event.

3.6.4 PEDESTAL TAB

When the Pedestals tab is active in the main window the mean value of the pedestal and noise for each channel is displayed (Figure 3.24). The noise is defined as the *rms* of the pedestal distribution.

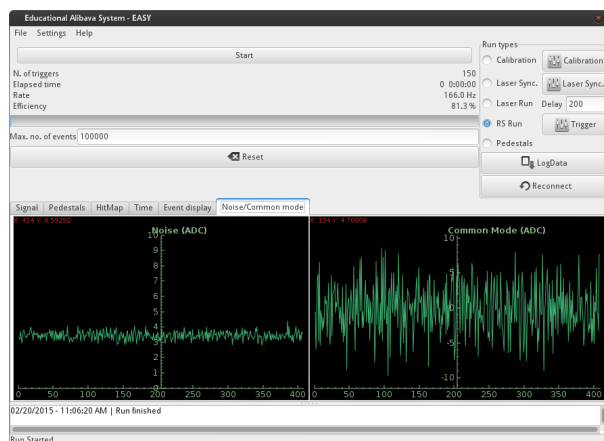


Figure 3.23.- Noise and Common noise event by event.

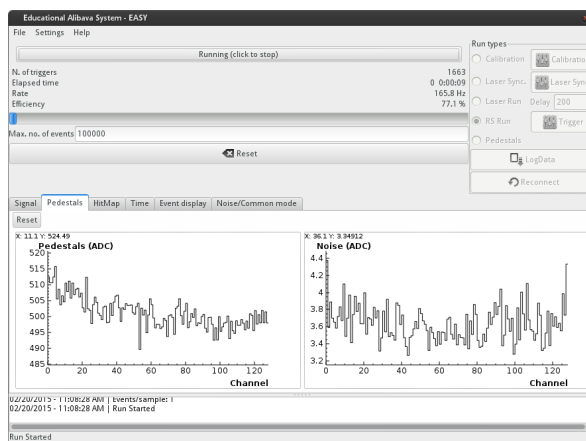


Figure 3.24.- Pedestal and noise for each channel.

3.7 CHANGING HISTOGRAM ATTRIBUTES AND HISTOGRAM PRINTING

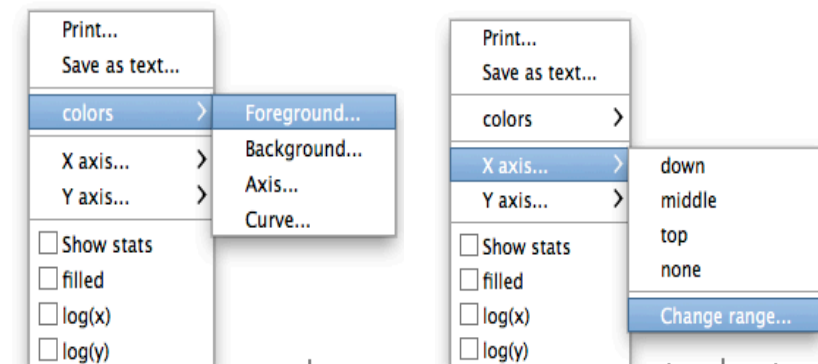


Figure 3.25.- Tabs to change the histograms attributes .

The user can change the histogram attributes by clicking on top of it with the mouse right button. A pop-up menu will appear as shown in Figure 3.25. Clicking on the *Print* item will let you save the histogram as a picture. You can also save it as text so that you can recover the curve with the program of your choice (*Save as text*).

Clicking on *colours* will allow you to change the background and foreground colours of the axis, the canvas and the histogram itself. You can also change the position of the axis, its range, set log scale, draw filled histograms or show the histogram statistics by activating the corresponding radio buttons. You can also change the range of the histogram axis to zoom a given region. This is done by selecting the zone to zoom with the left button of the mouse while pressing:

- CTRL for the X axis or
- SHIFT for the Y axis

3.8 THE HDF5 DATA FORMAT

In HDF5 the data is structured (Figure 3.25) in groups each one of them containing different information. There are 2 main groups:

- The header group contains general information about the run. It has the setup attribute that specifies the type of run and some other useful information, like the time of the acquisition. It also contains the pedestals and noise of each channel. There is a header group per run.
- The events group has four tables which contain the data collected for each event:
 - the charge deposition value on each channel,
 - the time of when the charge is sampled given by the TDC (see Figure 3.10),
 - the temperature (not measure in this version),
 - number of 40MHz clocks since the last reset of the Control Unit.

In the Calibration or Laser Scan runs the scan group contains the parameters of the run.

As an example, if a python program is used to access the data:

- The data file can be opened using `F=h5py.File(filename, 'r')`
- To read pedestals: `F['/header/pedestal']`
- To read noise: `F['/header/noise']`
- To read ADC charge: `F['/events/signal']`
- To read time of the ADC charge: `F['/events/time']`
- etc...

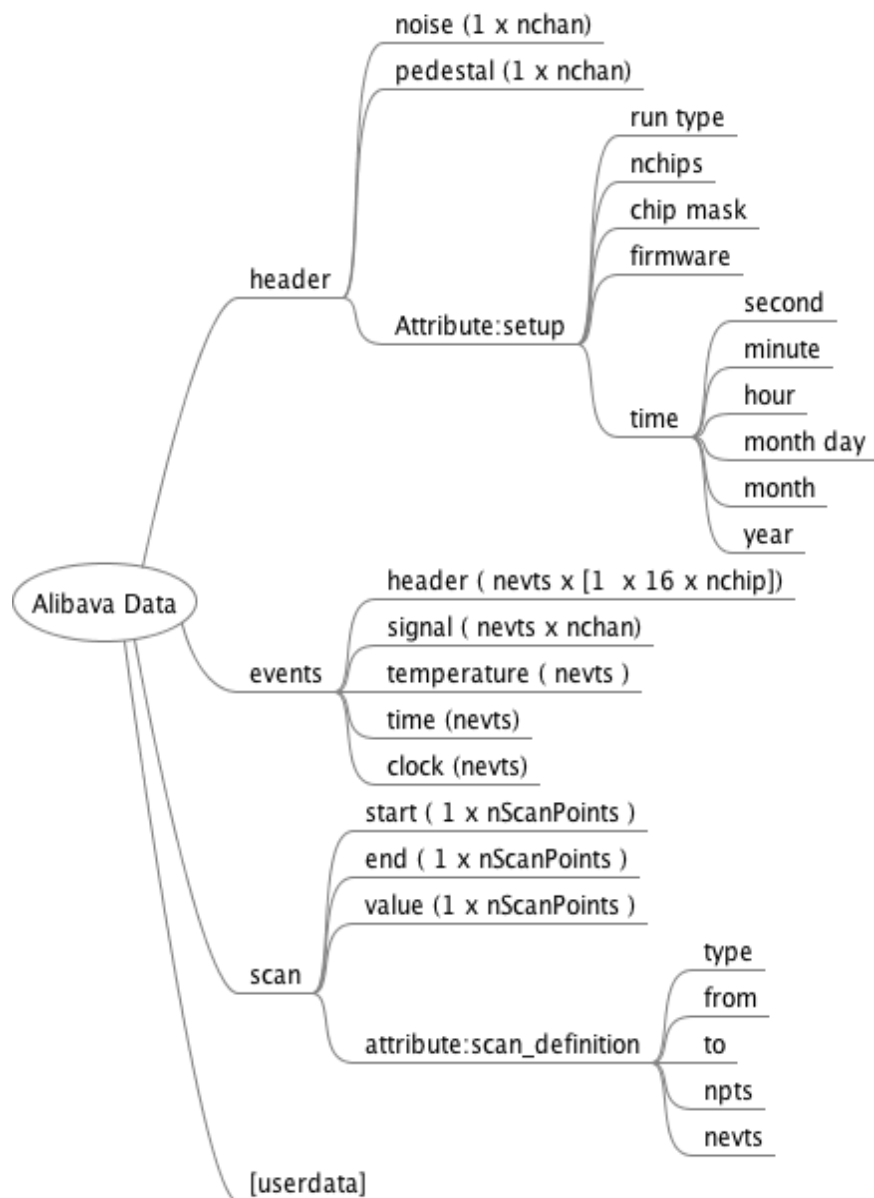


Figure 3.25.- HDF5 file data format.

4 EXERCISES

The EASY system illustrates the operation of a silicon strip detector with LHC readout electronics. The first exercise verifies the performance of the detector by measuring the leak current. The second exercise introduces the student to the concepts of pedestal, common noise and electronic noise. In the third exercise the student will learn about how to extract the signal from the energy deposition of a β source (Strontium-90). The fourth exercise is devoted to the synchronization of the Diode trigger signal. On the fifth exercise, the charge collected from a minimum ionization electron will be calculated. In the sixth exercise the student will calculate the depletion voltage from the Charge Collection Efficiency (CCE). In the seventh exercise the laser beam is used to demonstrate the strip structure of the detector. The eighth exercise introduces to the students the concept of space resolution assuming that there is and there is not charge sharing, digital and analogical readout. On the ninth exercise, the growth with depletion zone with bias voltage will be proved with the laser beam and the laser penetration will be calculated. And finally, in exercise ten, the self-trigger will be used to determinate the deposition energies of other kind of particles as gammas from Am-241 or Ba-133 or cosmic rays.

4.1 SETTING THE OPERATION VOLTAGE AND DETECTOR CURRENT.

The detector has to be fully depleted in order to deliver the full signal. The full depletion voltage depends on the resistivity of the material, the micro-strip sensor used in the EASY system has depletion voltage from 60V to 80V. It is advised to run at least 20V above full depletion, because a strong field speeds up the signal what is important when using fast electronics, since silicon detectors is basically a

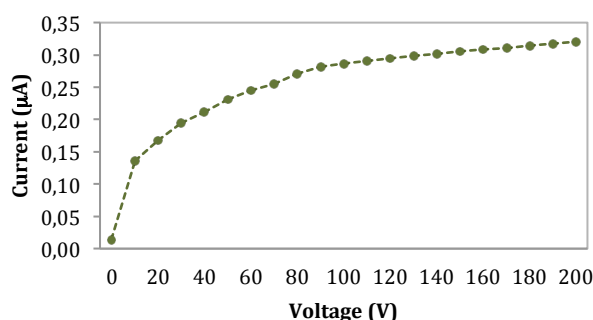


Figure 4.1.-Detector current as a function of the reverse voltage.

structured diode. The leakage current versus the bias voltage (IV curve) should show the typical diode behaviour. In practice, most detectors are not perfect and this is reflected in their current versus voltage curves.

A “perfect” detector shows a small rise in current at the beginning and then a long plateau up to the break through voltage. The small rise at the beginning is connected to the oxide charges. Some imperfections can cause the current to rise with voltage. Quite often, these increases are linear, i.e., resistive behaviour is observed. Imperfections on the p-side are immediately visible, while n-side imperfections only take effect after the detector is fully depleted.

We have to set up the operation voltage around 100V and make sure that the current at this operation voltage is not very high, typically below $2\mu\text{A}$. Figure 4.1 show the typical IV curve measured with the EASY system. Notice that the maximum current that the system is able to measure is $2.4\mu\text{A}$.

EXERCISE 1

IV CURVE:

- Connect the flat cable between the Control Unit and the Sensor Unit (section 1.2).
- Connect the USB cable between the Computer and the Control Unit (section 1.2).
- Power up the Control Unit (section 1.2).
- Apply bias voltage to the detector in 10V steps.
- Wait for a few seconds at each step and read the current.
- Plot the current as a function of the voltage (IV curve).
- Discuss the shape of the IV.
- Define the operation voltage well over the depletion voltage (e.g., 110V).

4.2 PEDESTAL, ELECTRONIC NOISE AND COMMON NOISE.

Before studying the charge formation in a silicon sensor, the student should understand the concept of pedestal, noise (it dependence with the reverse voltage bias) and the common noise. And therefore, the student will understand how the signal is defined from the raw data.

The pedestal value of the ADC output is an effective offset. Thus, for each channel the pedestal value is the measured ADC counts when there is no signal at the input. In the EASY system the ADC offset has been set to the mean range of the ADC, around 500 ADC counts, to allow read positive and negative signals, depending on the sensor type connected to the detector board, i.e, p-on-n silicon sensors collect positive signal (holes), as in the actual system, while n-on-p sensors collect negative signal (electrons).

When a particle passes through a detector, the trigger fires the acquisition, defining an event. The corresponding ADC count number (raw data) can be divided in three parts, and may be written as follows:

$$ADC(i, k) = P(i, k) + D(k) + \text{Signal}(i, k) \quad (14)$$

where i is the strip number and k the event number. $P(i, k)$ is the pedestal which fluctuates around a baseline. These fluctuations are due to electronic non-uniformities of each strip. $D(k)$ is the *common mode shift*, resulting for an electronic parasite pick-up which is specific of the chip and varies with time, fluctuating event by event. $\text{Signal}(i, k)$ represents the signal plus the residual noise and is deduced from $ADC(i, k)$, $P(i, k)$ and $D(k)$, as described in the section 4.3.

The first step in the study will be to calculate the pedestals and electronic noise, for that a pedestals run of N events will be started by selecting *Pedestals* in the *Run types* menu of the main window (Figure 3.1.a) and pressing the button *Start* as describe in section 3.3.3. To save the raw data, remember that the output file should be defined by selecting *LogData* before starting the run. While running the pedestals run, the students can observe the offset of the signals and their fluctuations by activating the *Event display* tab. During the acquisition the program makes an estimation of pedestals and noise that can be displayed by activating *Pedestal* tab of the main window (Figure 3.1.c).

During a pedestals run, we are measuring the output without injecting charge in the detector; we only have the pedestal value and the common noise (Equation 14). From this raw data the students can calculate pedestals, noise and common noise with a simple Python program (an example of analysis program, *EASY_Noise_Analysis.py* can be downloaded from <http://www.alibavasystems.com/> DOWNLOADS -> EASY).

In absence of signal, $\text{Signal}(i, k)=0$ (as is the case of a pedestals run), the pedestals are calculated as the mean value of the ADC (since the mean valour of the common noise is 0):

$$P(i) = \frac{1}{N} \sum_{k=1}^N ADC(i, k) \quad (15)$$

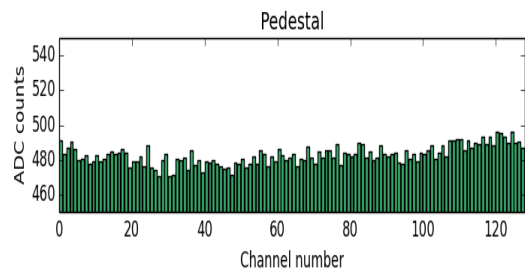


Figure 4.2.- Pedestal calculated from a pedestal run using the Python program.

Figure 4.2 shows the pedestal of each channel for a given run. Once the pedestals are determined for each channel, the common mode shift for a given event (k) is calculated for each event as the mean ADC charge of the 128 channels, after pedestal subtraction:

$$D(k) = \frac{1}{128} \sum_{i=1}^{128} (ADC(i, k) - P(i)) \quad (16)$$

Figure 4.3 shows the distribution of common noise, centred on zero as expected for large statistic, and the common noise event by event. Finally, the electronic noise of each channel is defined as the fluctuation of the pedestal after common noise subtraction. That is, the standard deviation (rms) of the pedestal after correcting for each event for the common noise, $P_c(i) = P(i) - D(k)$:

$$Noise(i) = \sqrt{\frac{1}{N-1} \sum_{k=1}^N (P_c(i) - \bar{P}_c(i))^2} \quad (17)$$

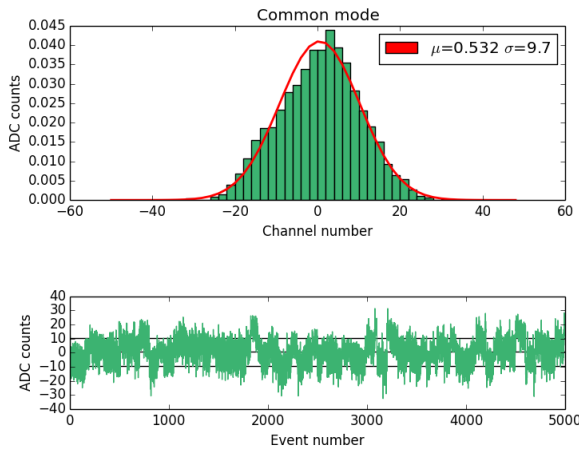


Figure 4.3.- Common noise distribution (top) and common noise event by event (bottom).

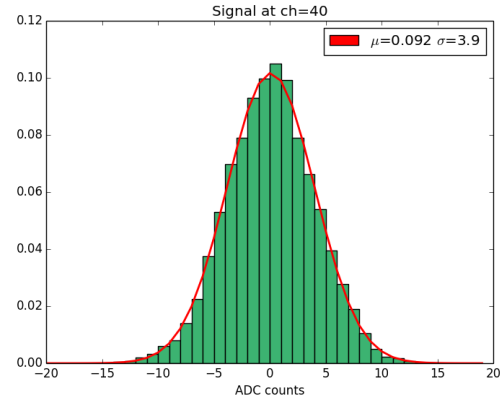


Figure 4.4.- Pedestal-Common noise distribution for channel 40 (normalize to 1). The rms of the distribution is the noise of the channel.

Figure 4.4 shows the noise for a given channel (channel 40) after pedestal and common noise subtraction, this magnitude follows a Gaussian distribution as expected for the electronic noise. The standard deviation of the distribution is the noise of the channel, 3.9 ADC units. The noise along the detector is presented in Figure 4.5, usually the noise increases in the detector borders.

As described in section 2.6, the electronic noise depends on the capacitance at the entry of the preamplifier, the shaping time, the resistances of the detector and of the readout chip, the temperature and the leaking current. The shaping time and the resistances are constants for a given device. Assuming that the temperature is kept constant, the student can study how the noise changes with the reverse depletion voltage of the detector and the relation with the detector capacitance and the leak current. Figure 4.6 shows the mean noise calculated over the full sensor (channels 1-128) and for the

central strips (channels 40-80) as a function of the reverse bias voltage for 1V to 100V.

The pedestals and noise can also be obtained directly from *Alibava-gui* as explained in previous sections, although it will be more instructive for the student to calculate those parameters from the raw data. The ways to get the pedestals and noise directly are:

- By using the *Saving as Text* by clicking over the histogram (see section 3.7).
- Saving the estimated noise and pedestal using the *Save Pedestal* (see section 3.4.8).

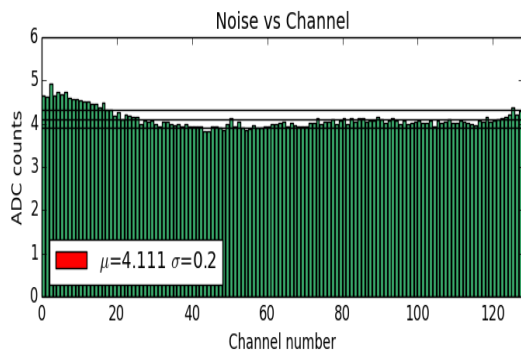


Figure 4.5.-Noise versus channel. The lines show the mean and rms of the noise distribution.

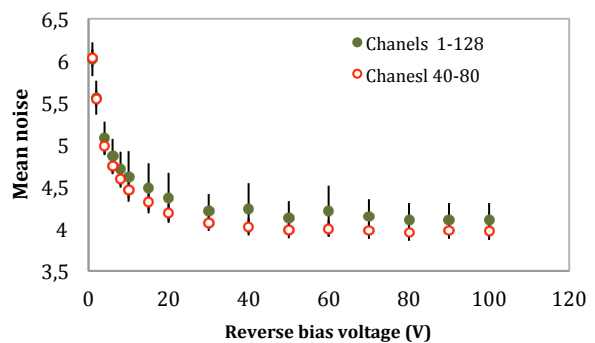


Figure 4.6.- Mean noise as a function of the reverse bias voltage for all channels and only for the central channels.

EXERCISE 2

PEDESTAL, ELECTRONIC NOISE AND COMMON NOISE

FROM RAW DATA:

- Connect the flat cable between the Control Unit and the Sensor Unit (section 1.2).
- Connect the USB cable between the Computer and the Control Unit (section 1.2).
- Power the Control Unit (section 1.2).
- Start *Alibava-gui* (section 3.2).
- Select the output file to log the raw data using the *LogData* in the main window
- Start a Pedestals run (section 3.3.3.)
- Look at the pedestals and noise histograms of the *Alibava-gui* (section 3.6.4).
- Discuss what is being shown.
- Using a Python program:
 - Define pedestals, common noise and electronic noise as explain in the text.
 - Calculate those magnitudes from the raw data.
 - Study the distribution of the electronic noise for a particular channel and discuss the Gaussian shape of the noise.
 - Study the distribution of noise over the detector.
- Take several runs increasing the reverse bias voltage slowly from 1V to 100V and calculate the mean electronic noise for each voltage.
- Comment what happens to the noise of the detector when the reverse bias voltage changes using the expression of ENC_{TOT} of equation (9).

FROM PEDESTALS AND NOISE obtained directly with *Alibava-gui*:

- Connect the flat cable between the Control Unit and the Sensor Unit (section 1.2).
- Connect the USB cable between the Computer and the Control Unit (section 1.2).
- Power the Control Unit (section 1.2).
- Start *Alibava-gui* (section 3.2).
- Start a Pedestals run (section 3.3.3.)
- Look at the pedestals and noise histograms of the *Alibava-gui* (section 3.6.4).
- Discuss what is being shown.
- Save the pedestals and noise by clicking over the histograms (as explain section 3.7) or using the *Save Pedestal* (see section 3.4.8).
- Calculate the mean noise from the text noise files.
- Take several runs increasing the reverse bias voltage slowly from 1V to 100V and calculate the mean electronic noise for each voltage.
- Comment what happens to the noise of the detector when the reverse bias voltage changes using the expression of ENC_{TOT} of equation (9).

4.3 SIGNAL, S/N RATE AND CLUSTER FINDING ALGORITHM.

When a particle crosses the detector, the sensor strips collect the charge deposition. For a given event, k , the signal on strip i is given by:

$$\text{Signal}(i, k) = \text{ADC}(i, k) - P(i) - D(k) \quad (18)$$

after pedestal ($P(i)$) and common noise ($D(k)$) subtraction.

When the charge arrives to a strip, the recorded signal will correspond to the collected charge and electronic noise, while the rest of the channels will record just the electronic noise. Figure 4.7 shows the raw data from the charge deposition of the minimum ionization (*MIP*) electrons from a Sr-90 source. In the histogram, all the 128 channels of the sensor have been considered. One can observe the noise is centred at zero with a Gaussian distribution and the charge deposition peaks at around ADC count (notice the logarithmic scale). The goal is to extract the deposited charge from the recorded signal in the recorded raw data.

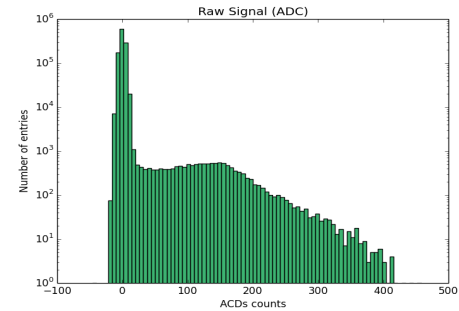


Figure 4.7.- Raw data signal distribution in ADC count after pedestal and common noise subtraction.

The first step to obtain the charge deposition is discriminating the channels with signal from those with only noise. The signal over noise ratio ($S/N(i, k)$) is used to define the relevant channels and discriminate them from the only-noise ones:

$$S/N(i, k) = \frac{\text{Signal}(i, k)}{\text{Noise}(i)} \quad (19)$$

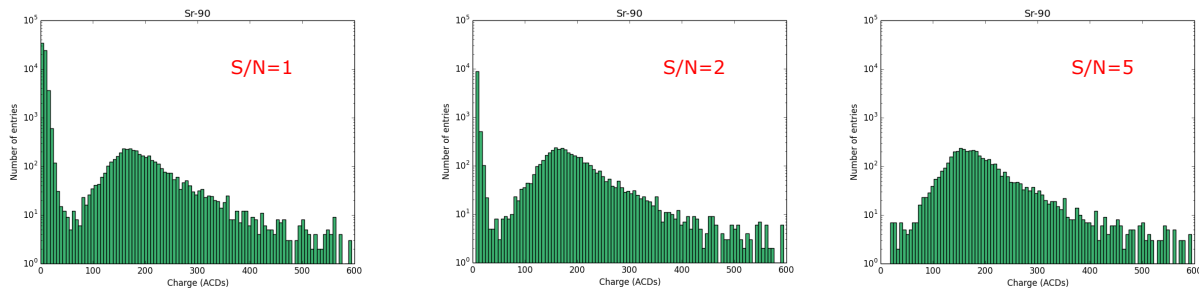


Figure 4.8.- Cluster energy using different S/N cuts .

Moreover, when a particle crosses the detector, the ionization produce drifts to the strips, and the charge can be shared amount several strips. A cluster algorithm has to be used to ensure that all the charge deposition is collected. For this exercise, we are using a very simple algorithm. The selection operates in the following steps:

- The strips are ordered in ascended strip number (from 0 to 127).

- Only the channels with a given S/N (i,k) over signal/noise cut (S/N_{cut}) are considered to reject noisy channels.
- The cluster search starts with the first strip (j) whose S/N (j,k) is over S/N_{cut} .
- If the next strip, $j+1$, has a signal larger than S/N_{cut} then strip $j+1$ is added to the cluster.
- The process continues until a strip below S/N_{cut} is reached.
- Every time a strip is included in the cluster it is marked as used to avoid being considered again.
- The cluster algorithm continues until all strips with $S/N(j,k) > S/N_{\text{cut}}$ are considered.
- The energy of a given cluster is defined as the sum of the charge collected by all the strips that constitute the cluster.

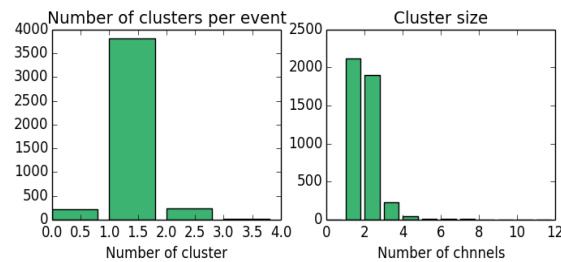


Figure 4.9- Number of clusters per event (left) and number of strips in a cluster (right).

Figure 4.8 shows the cluster energy reconstructed using different S/N_{cut} values. One can see how the noise decreases by increasing the cut in signal over noise and that for S/N_{cut} larger than 5 the distribution is free of electronic noise.

This simple cluster search algorithm allows having clusters with only one strip and more than one cluster per event. Figure 4.9 shows the histograms of the number of clusters in an event and the number of strips in a cluster for $S/N_{\text{cut}}=5$.

An example of analysis program, EASY_Charge_Analysis.py can be downloaded from <http://www.alibavasystems.com/> DOWNLOADS -> EASY.

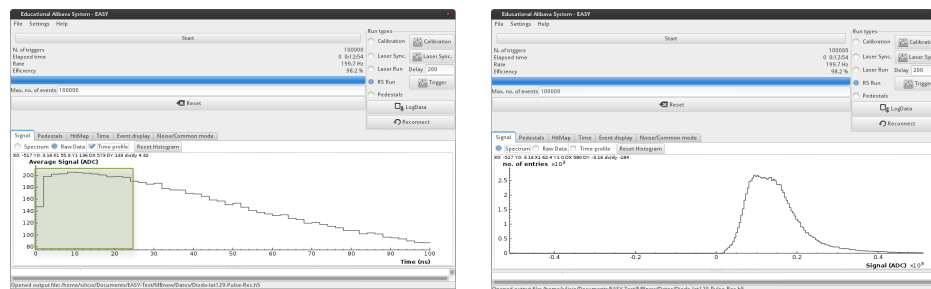
EXERCISE 3**SIGNAL, SIGNAL/NOISE RATIO AND CLUSTER FINDING ALGORITHM**

- Connect the flat cable between the Control Unit and the Sensor Unit (section 1.2).
- Connect the USB cable between the Computer and the Control Unit (section 1.2).
- Connect the LEMO cable between the Diode Trigger output of the Sensor Unit and the Single trigger jack of the Control Unit (section 1.2).
- Power the Control Unit (Section 1.2).
- Place a Sr-90 source over rectangular carbon fibre of the Sensor Unit aligned with the micro-strip sensor.
- Set detector bias voltage to 110V.
- Start *Alibava-gui* (Section 3.2).
- Select the diode trigger using:
 - Select *Pule In* trigger (section 3.4.4, Figure 3.13).
 - Set trigger threshold *Thrs+ Trigger Pulse In* to 50 mV and *Thrs- Trigger Pulse In* -50mV (section 3.4.4, Figure 3.13).
- Set latency to 129 (section 3.4.7.).
- Take a RS run saving the data to a file (remember to log the data file before starting the run).
- Analyse raw data by:
 - Define the signal/noise ratio.
 - Design a cluster finding algorithm.
 - Study the effect of the signal/noise ratio and the parameter of your cluster finding algorithm in total collected charge.
 - Select your signal over noise (S/N) working value.

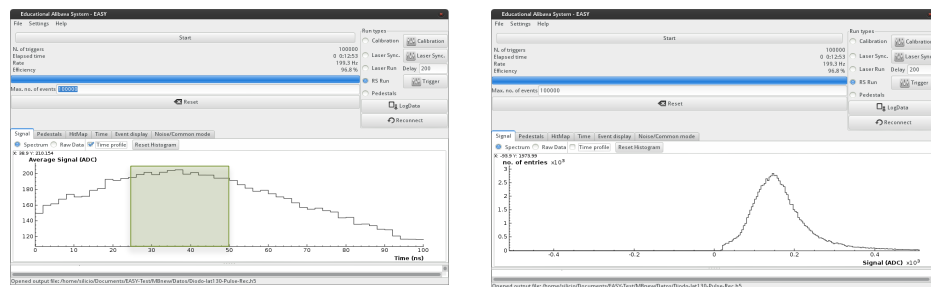
4.4 DIODE TRIGGER SYNCHRONIZATION AND PULSE RECONSTRUCTION.

The output signal of a silicon sensor is a short current pulse I_s (proportional to the particle energy deposition) with a signal duration of about 0.1 – 30 ns for a 10 – 500 μm thick sensor. In the EASY system the signal is read by the readout chip BEETLE, designed for the LHCb experiment. Therefore, the chip operates in the conditions of the Large Hadron Collider (LHC) with beams crossing every 25ns. The chip integrates the 128 channels of the sensor with low-noise charge-sensitive pre-amplifiers and shapers. For

Latency 129



Latency 130



Latency 131

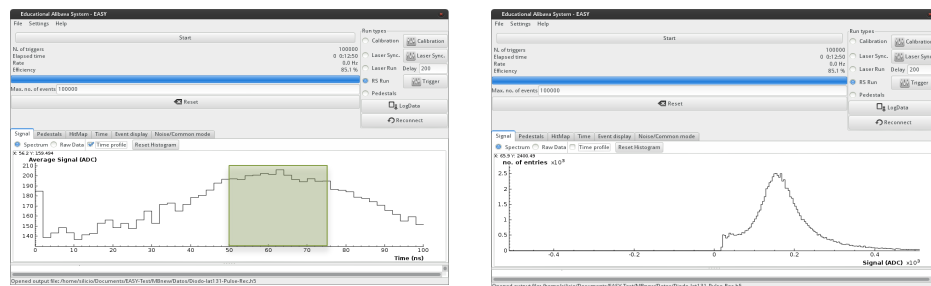


Figure 4.10.- Pulse reconstruction in the 100ns TDC window (left) and charge spectrum corresponding to this timing (right) for different latencies: top 129, middle 130 and bottom 131.

operation in the LHC, the pulse shape is chosen such that it complies with LHCb specifications: a peaking time of 25 ns with a reminder of the peak voltage after 25 ns of less than 30%. The shaping time is adjusted by programming the BEETLE frontend chip parameter V_{fs} (see BEETLE parameters in section 3.4.3). The shaper is sampled with the

LHC bunch-crossing frequency of 40 MHz into an analog pipeline. This ring buffer has a programmable latency of a maximum of 160 sampling intervals.

The trigger signal has to be synchronized with the pulse signal such that the signal will be sampled in its maximum to measure correctly the energy deposition of the particle. The diode trigger signal in our system has a large raising time (around 50ns) and large jitter. To ensure we sample the signal in its maximum, the output pulse of the silicon sensor is artificially enlarged using the V_{fs} parameter of the BEETLE, setting it to 150 as explained in section 3.4.3. This way, we broaden the maximum of the signal within the time window of the system (25ns) and then we ensure that the signal is sampled at its maximum.

In a RS (radioactive source) run, *Alibava-gui* allows the reconstruction of the pulse shape by measuring the signal as a function of the time between the rising edge of the 100ns clock signal and the trigger signal as shown section 3.4.3 (T1 in Figure 3.10). To carry out a pulse reconstruction, *Pulse Shape Rec* in the *DAQ general* configuration window has to be activated (see section 3.4.2, Figure 3.9). The pulse shape is displayed selecting *Time* profile in the display window after selecting the *Signal* tab, as explained in section 3.6.1.

Changing the latency of the BEETLE (section 3.4.3 or 3.4.7), the pulse can be moved in the 100ns time window, that way every time the latency increases in one unit the pulse will move 25ns to larger value of time. Figure 4.10 (left) displays the pulse shape reconstructed at latency values 129, 130 and 131, one can appreciate how the pulse moves in 25ns steps. The green area shows the 25ns window where the pulse reaches its maximum. The right side of Figure 4.10 shows the charge spectrum sampling over the full pulse spectrum displayed in the left side. For latency 129 (top of Figure 4.10), the charge spectrum is a superposition of landau distributions since the charge is sampled along the large tail of the pulse. The pulse is well centred in 100ns time window for latency 130, and the pulse distribution is more similar to a landau distribution. For latency 131 (bottom of Figure 4.10) we can appreciate the sampling before the arriving of the signal show as noise in the charge spectrum. Latency 131 is the closest approach to a perfect sampling, however we are still not sampling on the maximum of the pulse and the spectrum will not be a landau distribution. Therefore, to sample in the maximum of the pulse we have to restrict the TDC time valour of those of the green areas of Figure 4.10.

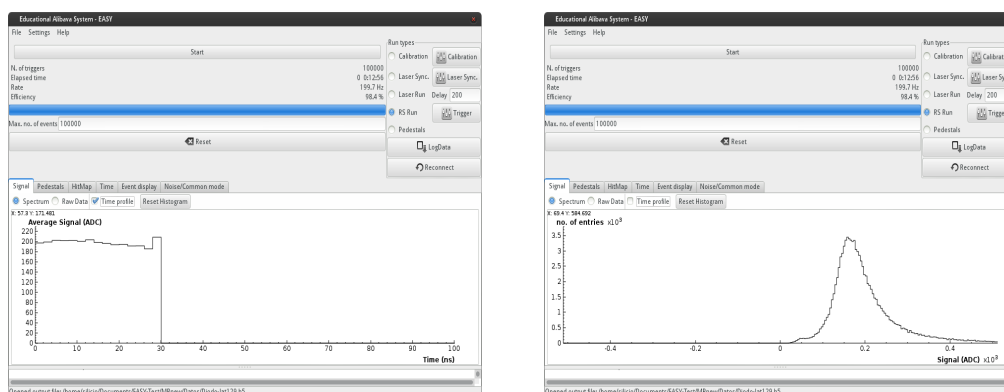


Figure 4.11.- Pulse reconstruction in the first 25ns window (left) and charge spectrum corresponding to this timing (right) for latency 129.

To speed the data acquisition up, one can restrict the timing only to the first 25ns, this is done if *Pulse Shape Rec* is not selected in the *DAQ* general window (as explained in section 3.4.2, Figure 3.9), to sample in the maximum of the distribution the 129 latency has to be selected. Notice how the charge spectrum improves in figure 4.11 where the data is restricted to the first 25ns.

EXERCISE 4

DIODE TRIGGER SYNCHRONIZATION AND PULSE RECONSTRUCTION

- Connect the flat cable between the Control Unit and the Sensor Unit (section 1.2).
- Connect the USB cable between the Computer and the Control Unit (section 1.2).
- Connect the LEMO cable between the Diode Trigger output of the Sensor Unit and the Single trigger jack of the Control Unit (section 1.2).
- Power the Control Unit (section 1.2).
- Place a Sr-90 source over rectangular carbon fibre of the Sensor Unit aligned with the micro-strip sensor.
- Set detector bias voltage to 110V.
- Start *Alibava-gui* (section 3.2).
- Select the diode trigger using:
 - Select *Pule In* trigger (section 3.4.4, Figure 3.13).
 - Set trigger threshold *Thrs+ Trigger Pulse In* to 50 mV and *Thrs- Trigger Pulse In* -50mV (section 3.4.4, Figure 3.13).
- Select *Pulse Shape Rec* is the *DAQ* general window (section 3.4.2, Figure 3.9)
- Take several RS runs to different latencies.
- Observe the pulse shape for the different latencies.
- Study the shape of the charge spectrum for the different latencies.
- Select the latency for which the maximum of the pulse is in first 25ns interval.
- Take a RS run without pulse reconstruction (deselect *Pulse Shape Rec* in the *DAQ* general window) and the selected latency to have the maximum of the pulse in the first 25ns.
- Study the shape of the charge spectrum.

4.5 CHARGE COLLECTION AND ENERGY DEPOSITION.

In previous exercises the student have learned how to extract the signal from the

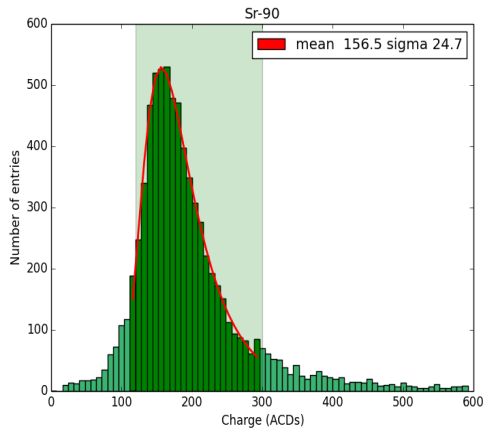


Figure 4.12.- Charge spectrum of a *MIP* electron crossing 300µm of silicon. The shadow area shows the interval use to feet to a Moyal function.

raw data and how to set up the parameters of the data acquisition to synchronize the acquisition with the trigger provided by the diode to sample the maximum of the signal. We are now in condition to calculate the energy deposition of *MIP* electron from the Sr-90 source in 300µm of silicon. The charge spectrum is a Landau distribution convolutes with a Gaussian distribution as explain in section 2.4. As a good approximation we are using a Moyal distribution. The Moyal distribution is a universal form for the energy loss by ionization for a fast charged particle and for the number of ion pairs produced in this process. The distribution was proposed by J. E. Moyal (*Moyal*) as a good approximation to the Landau distribution. The Moyal distribution is given by:

$$Moyal(\lambda) = \frac{1}{\sqrt{2\pi}} \exp \left\{ -\frac{1}{2}(\lambda) + e^{-\frac{1}{2}(\lambda)} \right\}$$

This analytical approximation is too low in the tail. In order to improve the fit, we define:

$$\lambda = \frac{x - m}{s} \quad (21)$$

with x being the dataset variable. m and s are fit parameters, and correspond to the mode and the width of the distribution. N is a normalization factor, so that the particular implemented formula is:

$$Landau(\lambda) = N Moyal(\lambda)$$

Figure 4.12 shows the charge spectrum with the fit to Moyal function. To improve the determination of the most frequent charge the fit has been restricted to the interval 120-300 ADCs. The most frequent charge deposition of a *MIP* electron crossing the 300µm micro-strip sensor is 156.5 ADCs.

The charge in ADC count can be converted into energy deposition using the calibration curve. The calibration curve depends on the BEETLE parameters and on the sensor voltage, therefore it has to be obtained in the same conditions as the charge spectrum. The process to obtain the calibration curve is described in section 3.3.1. Figure 4.13 shows a calibration curve to convert ADC counts to electrons (**notice that the calibration has to be done with Latency 128**, and set again to 129 for data acquisition). The calibration measures the Beetle amplifier response. One can observe the non-linear response of the amplifier. The maximum BEETLE range is a charge equivalent to 110.000 electrons. In a good approximation the curve of Figure 4.13 can be described as a fourth degree polynomial.

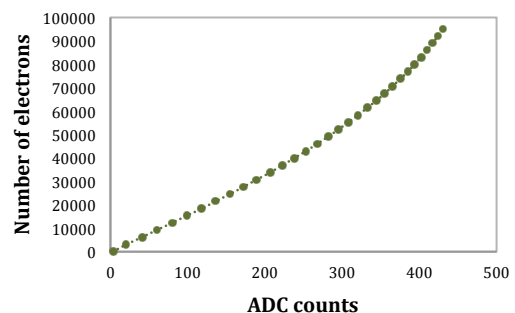


Figure 4.13.- Calibration curve to convert ADC count the electrons.

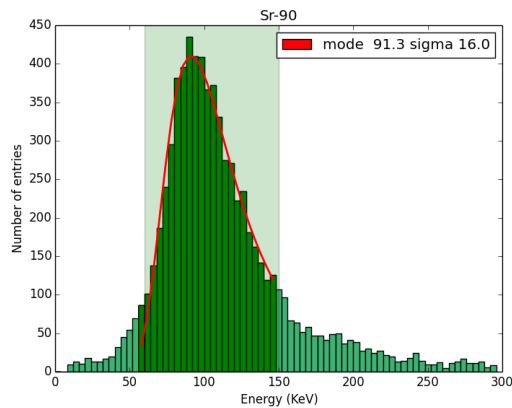


Figure 4.14.-Energy deposition of a *MIP* electron crossing 300μm of silicon.

$$N. \text{ electrons} = -124,089 + 142,381 \text{ ADC} + 0,2066 \text{ ADC}^2 - 0,8484 \cdot 10^{-3} \text{ ADC}^3 + 1,8303 \cdot 10^{-6} \text{ ADC}^4 \quad (22)$$

Equation 22 can be implemented in the analysis program to obtain the charge in number of electrons. In silicon, the energy required to produce an electron-hole pair is about 3.6 eV. Then, one can obtain that the most probable energy deposition of a *MIP* crossing 300μm of silicon is 91,3 KeV, as presented in Figure 5.14.

An example of analysis program, EASY_Charge_Analysis.py can be downloaded from <http://www.alibavasystems.com/> DOWNLOADS -> EASY.

EXERCISE 5

CHARGE COLLECTION AND ENERGY DEPOSITION

- Connect the flat cable between the Control Unit and the Sensor Unit (section 1.2).
- Connect the USB cable between the Computer and the Control Unit (section 1.2).
- Connect the LEMO cable between the Diode Trigger output of the Sensor Unit and the Single trigger jack of the Control Unit (section 1.2).
- Power the Control Unit (section 1.2).
- Place a Sr-90 source over rectangular carbon fibre of the Sensor Unit aligned with the micro-strip sensor.
- Set detector bias voltage to 110V.
- Start *Alibava-gui* (Section 3.2).
- Select the diode trigger using:
 - Select *Pule In* trigger (section 3.4.4, Figure 3.13).
 - Set trigger threshold *Thrs+ Trigger Pulse In* to 50 mV and *Thrs- Trigger Pulse In* -50mV (section 3.4.4, Figure 3.13).
- Select the latency following EXERCISE 4 and *Pulse Shape Rec.* deselected.
- Take a RS run saving the data to a file (remember do it before starting the run).
- Take a calibration run: delay and charge (section 3.3.1), saving the calibration curve
- Write an analysis program to extract the charge deposition (see EXERCISE 2 and 3), including:
 - Read Pedestals form the data file (estimated during data acquisition).
 - Calculate common mode noise for each event. This will be done as in ECERCICE 2, but without taking into account the strips with signal. In order to do this, calculate for every event the mean charge of all channels. Identify the channels with a charge value of more than 3 standard deviations from the mean. Finally, calculate again the mean charge without those channels. This will give you the common mode of the event.
 - Define a signal to noise cut and develop a cluster algorithm.
 - Obtain the charge deposition adding the charge of the channels in a cluster.
 - Convert the charge in ADC counts to energy using the calibration curve.
 - Process several events to obtain for charge spectrum.
 - Fit the charge distribution to a Moyal function and obtain the most probable charge.
 - Calculate the charge deposition of a *MIP* electron.

4.6 CHARGE COLLECTION EFFICIENCY (CCE) AND DEPLETION VOLTAGE.

When a charged particle crosses the micro-strip detector, the free charge carriers formed by ionization in the silicon will move in the detector field in the depleted part of the detector. This is because the ionization in the depleted region is not recombined and also accelerated by the electric field. While in the not depleted part, there is not electric field and charge will be reconvened. Therefore, only the charge generated in the depletion part will contribute to the signal.

The thickness of the depletion layer is proportional to $\sqrt{V/V_{dep}}$ (see equation 9). Hence for a uniform space charge in the detector, the induced charge will be also proportional to $\sqrt{V/V_{dep}}$. The Charge Collection Efficiency (CCE) is defined as the ratio of the collected

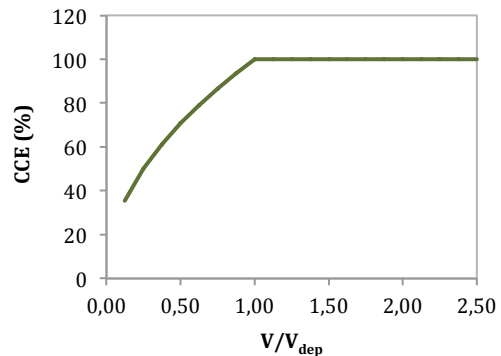


Figure 4.15.-Theoretical function of the Charge collection efficiency (CCE) as a function of the ratio V/V_{dep} .

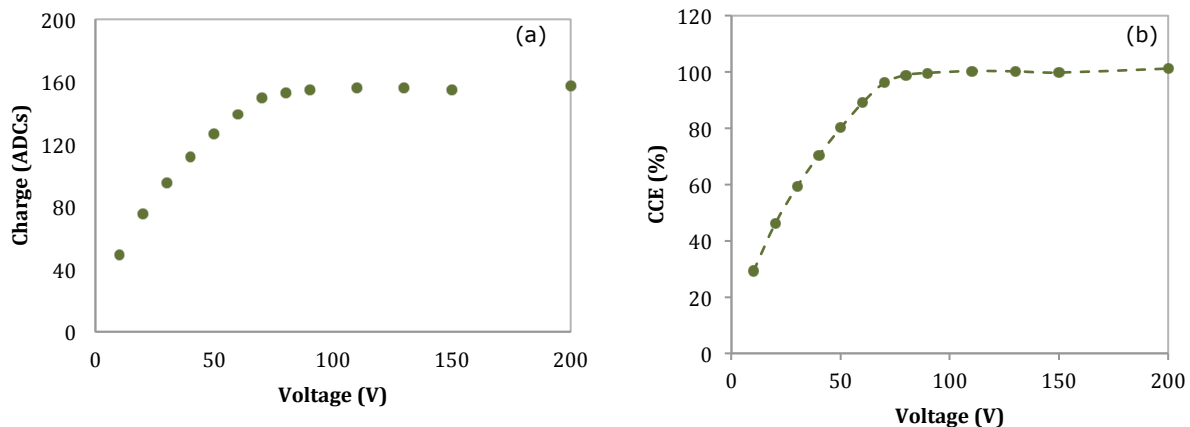


Figure 4.16.-Most probable charge as function of the bias voltage (a) and Charge Collection Efficiency (CCE) as function of the bias voltage (b).

charge over the collected charge when the detector is fully depleted. Figure 4.14 shows the theoretical prediction of the CCE as a function of V/V_{dep} . The CCE increases with the bias voltage reaching 100% when the detector is fully depleted

By measuring the collected charge of *MIP* electrons from a Sr-90 source as a function of the bias voltage, the CCE can be obtained to verify the theoretical prediction and to extract the depletion voltage (V_{dep}). Figure 4.16(a) shows the most probable charge obtained as explained in exercise 5 for different bias voltages. A signal over noise cut of 5 is applied, enough to discriminate charges above 20 ADC counts. The collected charge increases with voltage until it arrives to a plateau when the detector is fully depleted. The mean charge of the plateau is 155.5 ADC counts. The distribution can be normalized to the mean charge on the plateau to obtain the CCE (Figure 4.16(b)).

To extract the depletion voltage one can plot the square of CCE versus bias voltage and approximate the distribution with two straight lines, the intersection of those two lines will correspond to the depletion voltage as showed in Figure 4.17. The depletion

voltage obtained in this example was 76V. From the CCE we can calculate the depletion area width considering that the charge collected is proportional to the CCE and that a full depletion the 300 μ m of the sensor will be completely depleted. Figure 4.18 shows the depth of the depletion zone measurement from the p-n diode of the sensor top surface as a function of the bias voltage.

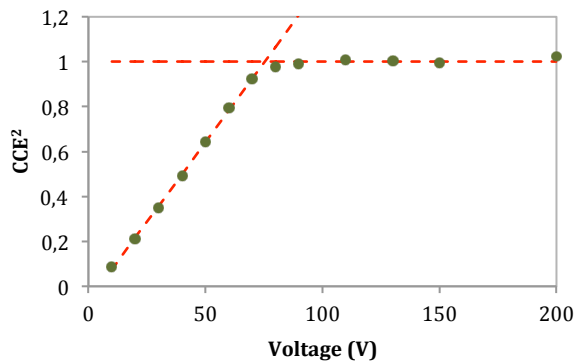


Figure 4.17.- CCE square versus bias voltage and fits to get the depletion voltage.

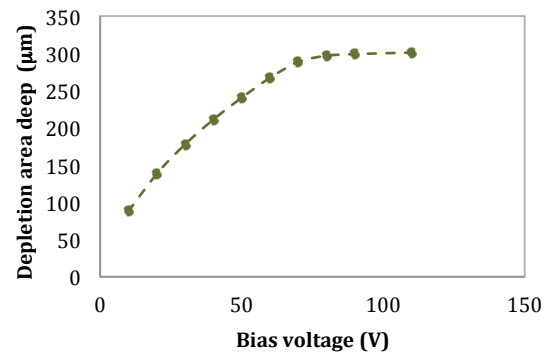


Figure 4.18.- Depletion area depth measurement from the p-n diode as a function of the bias voltage.

EXERCISE 6

CHARGE COLLECTION EFFICIENCY AND DEPLETION VOLTAGE

- Connect the flat cable between the Control Unit and the Sensor Unit (section 1.2).
- Connect the USB cable between the Computer and the Control Unit (section 1.2).
- Connect the LEMO cable between the Diode Trigger output of the Sensor Unit and the Single trigger jack of the Control Unit (section 1.2).
- Power the Control Unit (section 1.2).
- Place a Sr-90 source over rectangular carbon fibre of the Sensor Unit aligned with the micro-strip sensor.
- Set detector bias voltage to 110V.
- Start *Alibava-gui* (Section 3.2).
- Select the diode trigger using:
 - Select *Pule In* trigger (section 3.4.4, Figure 3.13).
 - Set trigger threshold *Thrs+ Trigger Pulse In* to 50 mV and *Thrs- Trigger Pulse In* -50mV (section 3.4.4, Figure 3.13).
- Select the latency following EXERCISE 4.
- Take several RS runes saving the data to a file (remember do it before starting the run), with different depletion voltage for example from 10V to 200V).
- Using the analysis program develop in EXERCISE 5, calculate the most probable charge for each bias voltage, and plot the results.
- Comment the shape of the distribution and compare with the theoretical distribution.
- Calculate the mean charge in the plateau and normalize the distribution to this value to obtaining de Charge Collection Efficiency (CCE).
- Extract the depletion voltage from the square of the CCE versus the bias voltage.
- Compare the result with the value from the sensor capacitance reported in section 2.3.
- Calculate the depletion depth as a function of the bias voltage.

4.7 STRIP STRUCTURE AND CHARGE SHARING.

The EASY system includes a pulsed laser to inject charge in the micro-strip detector in a controlled way, this will allow to study the strip structure of the detector and the way that charge is shared between strips.

To carry out the study, the first step is to synchronize the laser pulse with the acquisition. The synchronization of the laser is described in section 3.3.2, the timing of the maximum of the pulse should be introduced as an input in the box shown in Figure 3.7a.

Next, the laser should be focused using the two micrometric screws that move the laser up and down over the micro-strip detector (vertical screw) and in the horizontal

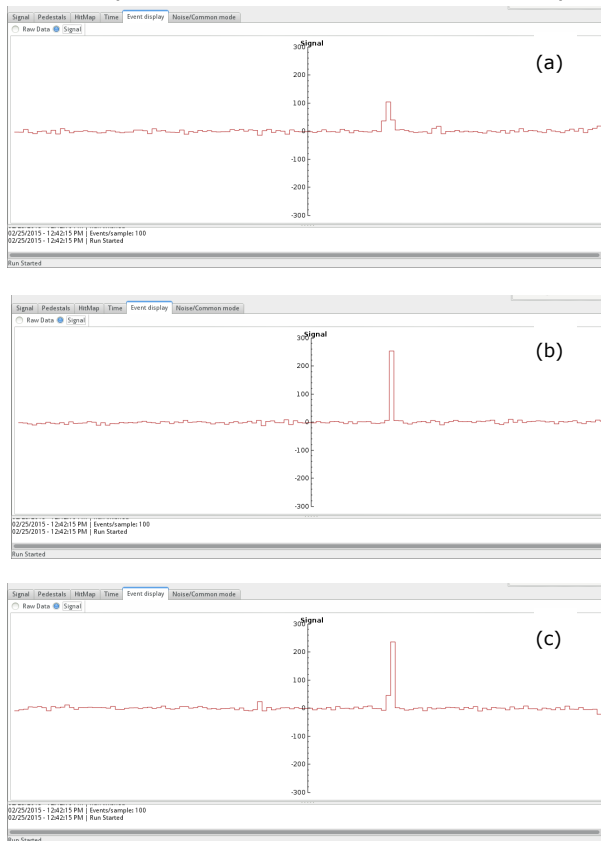


Figure 4.19.- Event display window at different steps of the process of the laser focusing: (a) initial display, (b) maximum of the signal and (c) strip structure.

From an initial position, take several laser runs moving the laser in the horizontal plane in steps of $10\mu\text{m}$. The distance between the centre of the strips (pitch) is $160\mu\text{m}$ and the strip width is $44\mu\text{m}$ as illustrated in Figure 4.20.

Figure 4.21 presents the charge collected for strips 39, 40 and 41 obtained by moving the laser perpendicular to them. Since the aluminium reflects the laser light, when the laser impacts on the strip no charge is collected in the strip, and the width of the strips can be calculated. By moving the laser away from the strip the charge on the considered strip reaches the maximum. Moving further, the charge in

plane, perpendicular direction of the strips (horizontal screw). The focusing is an iterative process. After, start the Laser run as described in section 3.3.4. The signal deposition should be observed by activation the *Event Display* tab. Move the two micrometric screws until a signal is observed in the Event Display window. Similar to the signal observed in Figure 4.19a. Then:

- Move up and down using the vertical screw until obtaining the larger signal.
- Move left and right using the horizontal screw until observe signal only in one strip (Figure 4.19b).
- With that we should have a good approximation to an optimum laser position, to confirm the focusing, move left or right the laser to observe that the signal moves from one strip to the next one (Figure 4.19c).
- Move the laser until getting a minimum of the signal due to laser incidence over the aluminium (the aluminium reflects the laser light), move the laser up and down until the laser signal disappears completely, this way we will be sure that the laser has been properly focused. If this is not observed, repeat previous steps.

Once the laser is properly focused, the study of the strips structure can be initiated.

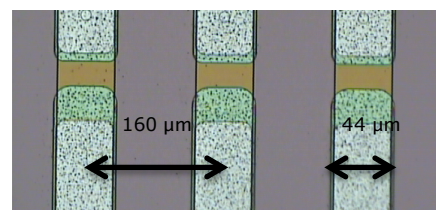


Figure 4.20.- Strip structure: pitch and strip width (aluminium strip).

the strip start decreasing and the neighbour strip starts collecting charge. This way, the charge sharing is illustrated. The pitch of the detector can be measured from the distance of the minimum of two adjacent channels. When the laser is over the strip, no signal is observed due to the laser reflexion in the aluminium and from the region without signal the width of the strip can be determined. Finally, the laser spot can be determined from the rising of the collected charge after the minimum of the signal (dark area in Figure 4.21), once the laser over pass the aluminium of the strip the charge begins to be injected in the detector until reaching the maximum. That corresponds to the total incidence of laser light in the detector.

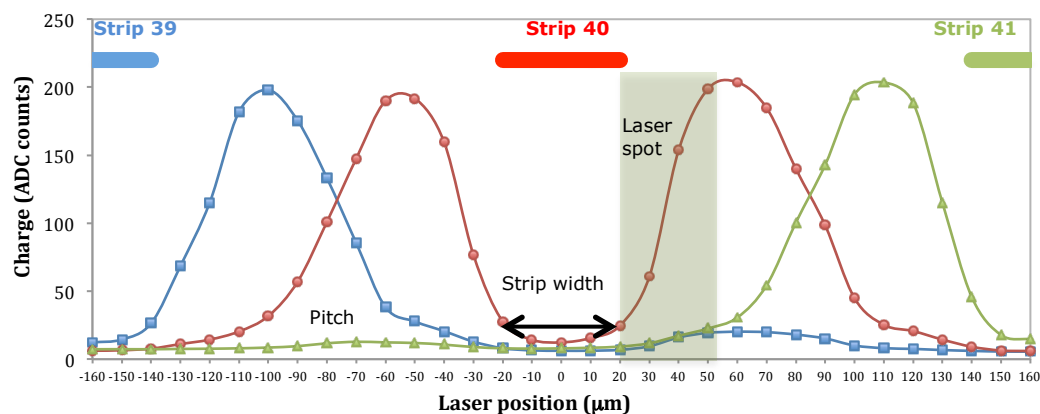


Figure 4.21. - Signal deposition of the laser charge in three consecutive strips obtained by moving the laser in 10 μ m steps perpendicular to the strips. The signal recorded by strip 39 is represented in blue, in red the signal in strip 40 and in green the signal in strips 41. In the top of the figure the strip structure is represented.

An example of analysis program, EAST_Laser_Scan_Analysis.py can be downloaded from <http://www.alibavasystems.com/> DOWNLOADS -> EASY.)

EXERCISE 7

STRIP STRUCTURE AND CHARGE SHARING

- Connect the flat cable between the Control Unit and the Sensor Unit (section 1.2).
- Connect the USB cable between the Computer and the Control Unit (section 1.2).
- Connect the optical fibre between the Sensor Unit and the Control Unit (Section 1.2).
- Power the Control Unit (section 1.2).
- Set detector bias voltage to 110V.
- Start *Alibava-gui* (section 3.2).
- Synchronize the laser (section 3.3.2) and set up the laser delay.
- Start a large laser run and focus the laser as described previously.
- Once the laser is properly focus. Take several Laser runs saving the data to a file (remember do it before starting the run), moving the laser in 10 μ m steps perpendicular to the strip direction (horizontal screw). Cover at least a distance of 320 μ m (twice the detector pitch)
- Using an analysis program read the signal of the scanned strips and plot the charge as a function of the laser position for the scanned strips.
- Comment the shape of the distribution.
- Calculate the width of the strip and the detector pitch.
- Calculate the laser spot.
- Comment how the charge is shared between neighbour channels when the laser light falls in the inter-strip region.

4.8 SPATIAL RESOLUTION: BINARY VS ANALOGICAL READOUT.

Micro-strip silicon detectors are position detectors; they are able to provide high-resolution information about where particles passed through the sensor. Their intrinsic resolution depends mainly on the pitch and whether digital or analogue readout information is used.

If the charge of a traversing particle is not shared between strips the resolution is binary and dominated by the strip pitch according to equation:

$$\sigma^2 = \frac{1}{p} \int_{-p/2}^{p/2} (x - \langle x \rangle)^2 dx = \frac{p^2}{12} \rightarrow \sigma = \frac{p}{\sqrt{12}} \quad (23)$$

If there is charge induced on the neighbouring strips depends only on the linear distance from the strip, the use of centre-of-gravity- or so-called η -algorithms is allowed, and the reconstructed position can be calculated as:

$$x_r = x_L + \frac{ADC_R}{ADC_R + ADC_L} p \quad (24)$$

When the ADC_R and ADC_L are the charge induced in the strips to the right and left of the incident position and x_L the position of the left adjacent strip. The ratio:

$$\eta = \frac{ADC_R}{ADC_R + ADC_L} \quad (25)$$

is called the *eta function*. The spatial resolution is dependent on the ADC/Noise ratio, where ADC is the most probable charge (153 ADC counts for a *MIP* electron using the standard Beetle parameters) and the detector pitch according to the approximation for a lineal distribution of charge:

$$\sigma \approx \frac{p}{ADC/Noise} \quad (26)$$

To study the spatial resolution with the EASY detector, only two of the strips of EXERCISE 7 are going to be considered, strips 39 and 40. We take the following convention: the centre of strip 39 is place at $-160\mu\text{m}$ and centre of strip 40 at $0\mu\text{m}$. In contrast to laser light, charged particles will not reflex in the aluminium of the detector. To extrapolate the laser data to the data from a charged particle we have to assume:

- The charge deposition on the region will be the same as the maximum charge obtained with the laser (zone 1 in Figure 4.22a).
- There is no effect of the laser beam spot, so the charge will also be the maximum charge on this region close to the strip (zone 2 in Figure 4.22a).
- Finally, the laser charge deposition has to be normalized to the corresponding charge of a *MIP* electron at full depletion obtained in EXERCISE 5 (156 ADC counts).
- Only Signal/Noise larger than 5 will be considered which correspond to 20 ADC counts in our case.

Figure 4.22a shows the collected charge using the laser beam (EXERCISE 7) with narrow dotted line and the assumed collected charge of a *MIP* charge particle with wide solid lines.

The laser incident position will be considered as the nominal position (x_n), the reconstructed position (x_r) will be calculated considering three cases:

- (a) **Pure Binary readout**, so the reconstructed position will be the position of the centre of the strip with larger charge collected ($-160\mu\text{m}$ or $0\mu\text{m}$ for the strips 39 and 49).
- (b) **Binary readout with charge sharing**, if there is only charge in one strip the reconstructed position will be the corresponding strip position ($-160\mu\text{m}$ or $0\mu\text{m}$), if there is charge in both strips the reconstructed position will be the inter strip position ($-80\mu\text{m}$).
- (c) **Analog readout**, the reconstructed position will be obtained using equation (24).

The residual is defined as the difference between the nominal position and the reconstructed position ($r = x_n - x_r$), the resolution will be given by the rms of the residual.

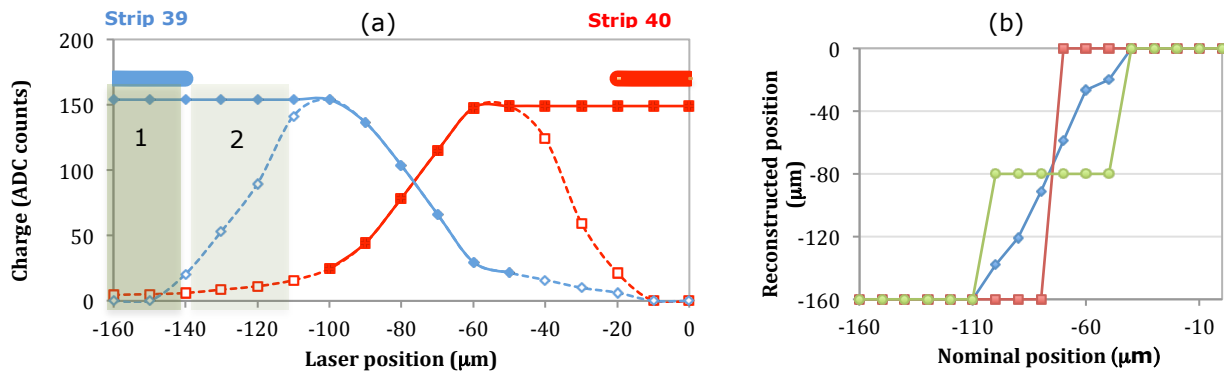


Figure 4.22.- (a) Charge collected by strips 39 and 40 versus incident position of a MIP charge particle obtained by extrapolation the result of EXERCISE 7 using a laser beam. (b) η -function for the three cases considered in the text: (red) pure binary readout, (green) binary readout with charge sharing and (blue) analogy readout.

Table 1.4 shows the reconstructed and the residual positions considering the three previous cases, for case (a) the spatial resolution is $46,11\mu\text{m}$ coherent with the expected value of $p/\sqrt{12}=46,2\mu\text{m}$ for a $160\mu\text{m}$ pitch detector. The resolution improves using case (b) and case (c). However, since the charge sharing is not linear between strips due to the large pitch of the detector, the resolution in case (c) does not improve drastically. Figure 4.21b shows the reconstructed position as a function of the nominal position for the three cases.

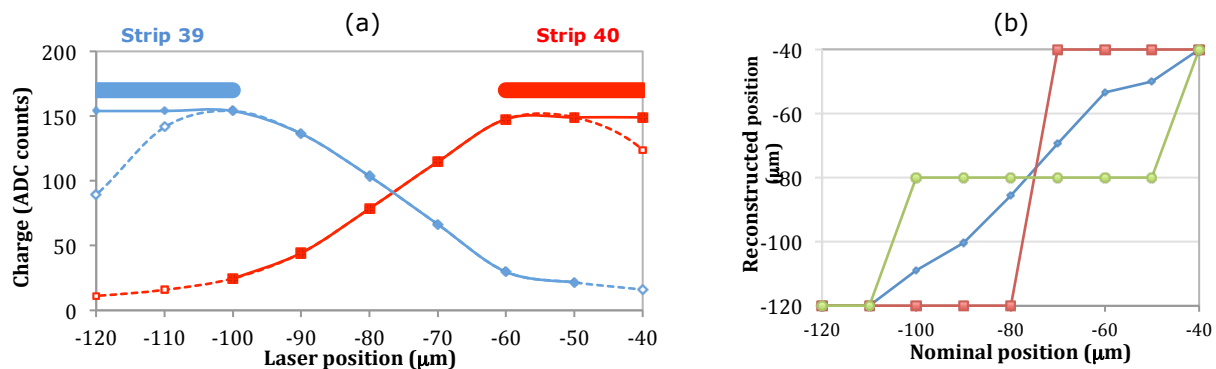


Figure 4.23.- (a) Charge collected by strips 39 and 40 versus incident position of a MIP charge particle obtained by extrapolation the result of EXERCISE 7 using a laser beam and a pitch of $80\mu\text{m}$. (b) η -function for the three cases considered in the text: (red) pure binary readout, (green) binary readout with charge sharing and (blue) analogy readout.

Table 1.4.- Data used to obtain the detector resolution for a 160 μ m pitch detector.

PITCH 160 μ m			DIGITAL READOUT				ANALOGIC READOUT	
x_n (μ m)	Charge strip 39 (ADCs)	Charge strip 40 (ADCs)	x_r (μ m) (a)	r (μ m) (a)	x_r (μ m) (b)	r (μ m) (b)	x_r (μ m) (c)	r (μ m) (c)
-160		153,9	-160	0	-160	0	-160	0
-150		153,9	-160	-10	-160	-10	-160	10
-140		153,9	-160	-20	-160	-20	-160	20
-130		153,9	-160	-30	-160	-30	-160	30
-120		153,9	-160	-40	-160	-40	-160	40
-110		153,9	-160	-50	-160	-50	-160	50
-100	24,6	153,9	-160	-60	-80	20	-138	38
-90	44,3	136,5	-160	-70	-80	10	-121	31
-80	78,5	103,6	-160	-80	-80	0	-91	11
-70	114,7	66,4	0	70	-80	-10	-59	-11
-60	147,7	29,7	0	60	-80	-20	-27	-33
-50	149,0	21,6	0	50	-80	-30	-20	-30
-40	149,0		0	40	0	40	0	-40
-30	149,0		0	30	0	30	0	-30
-20	149,0		0	20	0	20	0	-20
-10	149,0		0	10	0	10	0	-10
0	149,0		0	0	0	0	0	0
MEAN (μ m)				-4,71		-4,71		3,26
RMS(μ m)				46,11		25,03		28,45

Looking at the Figure 4.22b for analogical readout (blue line), one can appreciate that the detector pitch has not been optimized to obtain the best resolution using the charge sharing information. To get a linear charge sharing between strips, the strip 39 should be placed at -120 μ m (central strip position) and strip -40 μ m, therefore the optimum pitch of the detector should be 80 μ m. We are assuming the electrical field in the detector will be the same for 160 μ m and 80 μ m pitch. With these assumptions we can calculate again the resolution for the three cases considered. Figure 4.23a shows the new strip position and the charge sharing between them. Table 1.5 presents the new reconstructed position and residuals for the three cases considered, Again for case (a) we have a good agreement between the resolution obtained and the expected value, $p/\sqrt{12}=23,1\mu$ m for a 80 μ m pitch detector. The resolution improves also for case (b). However, the improvement for case (c) is huge due to the lineal charge sharing, the expected value for equation (26) is around 10 μ m ($p/156/20$).

Table 1.5.- Data used to obtain the detector resolution for a 80 μ m pitch detector.

PITCH 80 μ m			DIGITAL READOUT				ANALOGIC READOUT	
x_n (μ m)	Charge strip 39 (ADCs)	Charge strip 40 (ADCs)	x_r (μ m) (a)	r (μ m) (a)	x_r (μ m) (b)	r (μ m) (b)	x_r (μ m) (c)	r (μ m) (c)
-120		153,9	-120	0	-120	0	-120	0
-110		153,9	-120	10	-120	10	-120	10
-100	24,6	153,9	-120	20	-80	-20	-109	9
-90	44,3	136,5	-120	30	-80	-10	-100	10
-80	78,5	103,6	-120	40	-80	0	-86	6
-70	114,7	66,4	-40	-30	-80	10	-69	-1
-60	147,7	29,7	-40	-20	-80	20	-53	-7
-50	149,0	21,6	-40	-10	-80	30	-50	0
-40	149,0		-40	0	-40	0	-40	0
MEAN (μ m)				4,44		4,44		3,08
RMS(μ m)				22,97		15,09		5,89

EXERCISE 8**SPATIAL RESOLUTION: BINARY VS ANALOGICAL READOUT**

- Using the data of EXERCISE 7 for two adjacent strips, discuss what the differences are between the laser data and the MIP data.
- Convert the laser data in the data from a MIP particle, correct for the effect of the reflexion in the aluminium strip, correct for the effect of the laser beam spot, assume the charge collected for a MIP from EXERCISE 5 and the Signal/Noise cut.
- Define different algorithms to reconstruct position of an incident particle and the associated residuals to obtain the resolution, for example:
 - Pure Binary readout: the reconstructed position will be the position of the centre of the strip with larger charge collected.
 - Binary readout with charge sharing: the reconstructed position will be, if there is only charge in one strip the corresponding strip position, if there are charge in both strip the reconstructed position will be the inter strip position.
 - Analogical readout: the reconstructed position will be obtained using centre-of-gravity- or so-called η -algorithms.
- Compare the resolution obtained with the expected resolution.
- From the previous result, define the optimum pitch of the detector.

4.9 LASER PENETRATION IN SILICON.

The growth of the depletion zone with the bias voltage can be proved using the laser light by recording the charge collected for various voltages. The measured charge will be a convolution of the extension of the depletion zone and the energy deposition within the silicon. In the case of *MIPs*, as EXERCISE 6, which deposit the energy uniformly in the silicon, the measured charge is proportional to $\sqrt{V/V_{dep}}$. For a laser light pulse, the energy deposition is exponential and given by:

$$E(y) = E_0 \left(1 - e^{-y/a}\right) \quad (27)$$

where y is the distance perpendicular to the silicon detector and its origin is located at the surface where the laser enters in the detector, and a is the penetration depth of the laser light in the silicon, which depends on the laser wavelength. Therefore, for a given laser light, the charge collection curve will depend on the depth of the depletion area but also on the energy lost (e.i. on the laser wavelength, the higher the wavelength the faster rise with the bias voltage (*Abt*)).

The penetration of laser in silicon has been measured for some wavelengths, for example, for the 960nm the penetration is around 74 μ m and for 1037nm is 380 μ m (*Lide*). The laser of the EASY system has a wavelength of 980nm, a priori; its penetration in silicon is unknown.

The charge detected will depend on the charge deposited in the depleted area. The CCE as a function of the bias voltage (V) will be given by:

$$CCE(V) = \frac{(1 - e^{-d(V)/a})}{(1 - e^{-300/a})} \quad (28)$$

Where d is the depletion area width. From EXERCISE 6, one can obtain $d(V)$ as plotted on Figure 4.18. Figure 4.24 represents the CCE for different laser penetrations together with the *MIP* data from EXERCISE 6. For laser penetration larger than 1mm the laser data is a good approximation to a *MIP*.

EXERCISE 7 explains how to start and focus the laser. After focusing and placing the laser in a fixed position, the charge collected for different bias voltages can be recorded and analysed as the *MIP* data of EXERCISE 6. Note that for laser data, *Alibava-gui* is not able to do a proper calculation of data and pedestals, so before starting the laser data acquisition take a dedicated pedestals run and give pedestals and noise as input to the analysis program.

An example of analysis program to get the charge collected for each voltage, `EASY_Laser_Charge_Analysis.py` can be downloaded from <http://www.alibavasystems.com/> DOWNLOADS -> EASY. From the charge collected versus bias voltage, the CCE is calculated.

On Figure 4.25, the data collected with Laser light is presented together with the *MIP* data from EXERCISE 6. By comparing the laser and the *MIP* data one can conclude that the laser stops inside the detector. By fitting data to equation (28), using the calculation of the depletion depth as a function of the bias voltage from EXERCISE 6, one can obtain the laser penetration $a = 167\mu$ m. Figure 4.25 shows the fitting curve.

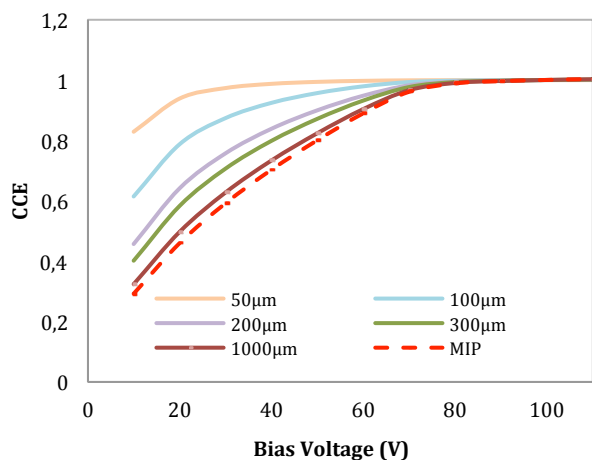


Figure 4.24.—Theoretical Charge Collection Efficiency for different laser penetrations in silicon and data for a MIP electron calculated in EXERCISE 6.

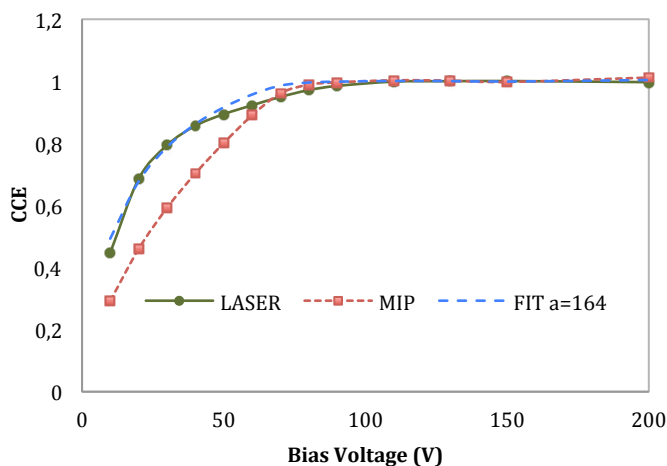


Figure 4.25.—Charge Collection Efficiency from laser data, fit to a penetration length of 167μm and data for a MIP electron calculated in EXERCISE 6 for comparison

EXERCISE 9

LASER PENETRATION IN SILICON

- Connect the flat cable between the Control Unit and the Sensor Unit (section 1.2).
- Connect the USB cable between the Computer and the Control Unit (section 1.2).
- Connect the optical fibre between the Sensor Unit and the Control Unit (Section 1.2).
- Power the Control Unit (section 1.2).
- Set detector bias voltage to 110V.
- Start Alibava-gui (Section 3.2).
- Synchronize the laser (section 3.3.2) and set up the laser delay.
- Start a large laser run and focus the laser as described in EXERCISE 7.
- Once the laser is properly focus fix the laser position. Take several Laser runs changing the bias voltage, saving the data to a file (remember do it before starting the run).
- Read the charge collected for each bias voltage using an analysis program.
- Plot the collected charge, bias voltage and compare with the plot obtained with the Sr-90 source. Comment the different shapes and discuss the origin of the differences.
- Using the calculated depletion zone depth from EXERCISE 6 and equation (28), fit the data to obtain the laser penetration. Plot the fitted curve.

4.10 SPECTROSCOPY USING SELF-TRIGGER.

The BEETLE ASIC incorporates a self-trigger signal that will be issued whenever one of its 128 channels registers a signal larger than a preprogrammed threshold. To accomplish that, the incoming signal is split into two branches. One goes through a shaper and then to a comparator that will issue the trigger signal for values above a threshold. The signal of the second branch is used to measure the generated charge in the detector.

The Self-Trigger mode allows measuring the charge induced by particles crossing the detector but also photons or alpha particles absorbed in the detector. The range of the ADC incorporated in the Control Unit and the dynamic range of the BEETLE define the upper energy limit the system can measure. The low energy ranges will be defined by the noise of the system. Typically, the energy range goes from 20KeV to 300KeV.

Before starting the system, the LEMO jack of the Self-Trigger of the Sensor Unit has to be connected to the LEMO jack of the single trigger signal (*Pulse*) to transmit the trigger signal. Once the trigger cable is connected and the detector bias is set to 100V, the crucial step is the calibration to fix the threshold of each channel as explained section 3.5 (make sure that the trigger signal is connected and the detector bias to the operational voltage). After running the calibration, press *ok* and download the calibration file with the extension ".ini" as explained in section 3.5.

Before initiating the data acquisition, the calibration file has to be loaded to set the threshold and activate the comparator (BEETLE parameter *CompCtrl* will be set automatically to 15 to activate the comparator). To check the threshold, select *Comparator Setting* in *Setting* (see section 3.4.5) and mark *Channel Thrs. Coor.*

Select the trigger configuration: *Pulse In trigger* (section 3.4.4, Figure 3.13) and set trigger threshold *Thrs+ Trigger Pulse In* and *Thrs- Trigger Pulse In* to 500 mV and -500mV (section 3.4.4, Figure 3.13).

The system has to be synchronized by selecting the proper BEETLE *Latency*. In contrast to case of the Diode trigger, we cannot use the TDC information, so we will place the Sr-90 source in the Sensor Unit and we will take data scanning over the different value of Latency (128 and forwards). When the same or a similar signal to the one obtained with the Diode trigger is observed, we will fix the Latency (usually Latency=135).

Notice that for some values close to the correct latency, a charge distribution can be obtained, however it is not in the right position due the signal out of time signal an also large noise.

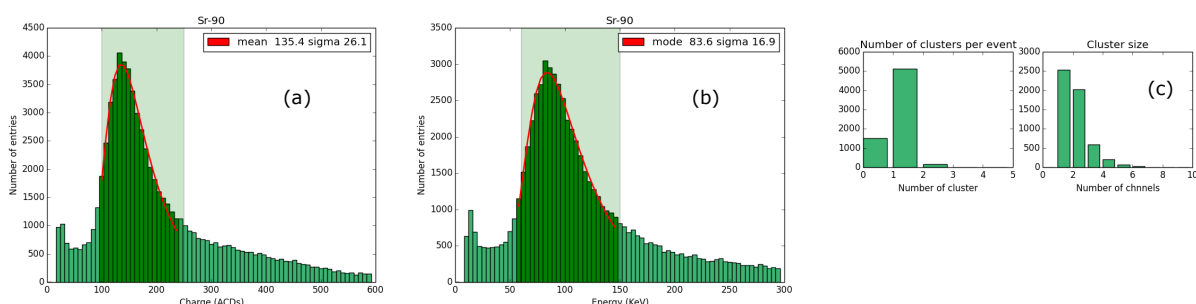


Figure 4.26.- Charge collected from Sr-90 source in ADC counts (a) and in energy (b). On (c), the number of cluster per events and the number of strip per cluster are represented.

Once the Latency is fixed, the data can be recorded and analysed using the same analysis program as EXERCISE 6. Figure 4.26a shows the charge distribution in ADC

counts, similar to the distribution of Figure 4.12 for the Diode trigger. The differences between the two spectrums are due to the fact the Self-trigger is also sensible to electrons that stop in the silicon (the energy spectrum of the electrons from Sr-90 is continuous, rising from zero until the endpoint at 546KeV (Mante)).

Figure 4.26c presents the number of clusters per event and the number of strips per cluster are to be compared with Figure 4.9 for the Diode Trigger. The Self-Trigger is a bit less efficiently since more events have zero clusters. The distribution of strips in a cluster is very similar for both triggers and corresponds to the expected inducing signal of electrons crossing a silicon strip detector.

The collected charge can be converted to energy using the calibration curve of the BEETLE. Notice that the calibration (section 3.3.1) depends on the chip parameters, so a specific calibration has to be taken when using the Self-trigger. The energy deposition of the electron from the Sr-90 source is plotted in Figure 4.26b.

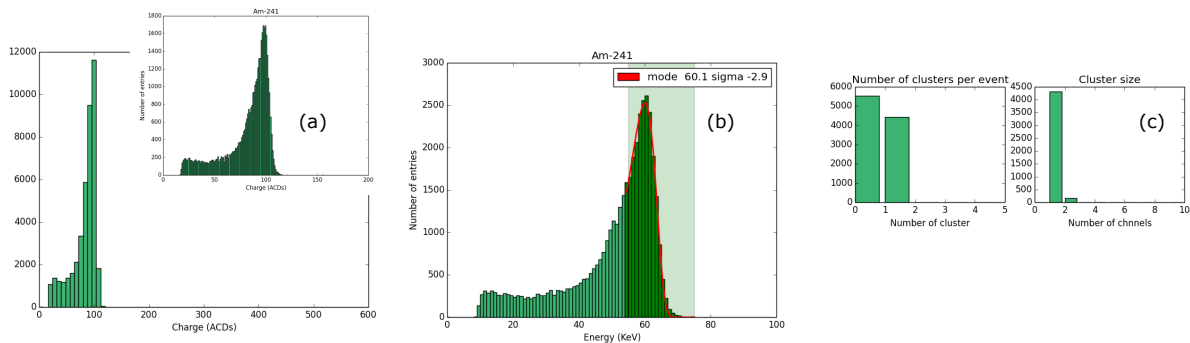


Figure 4.27.- Charge collected from Am-241 encapsulated source in ADC counts (a) and in energy (b). On (c), the number of cluster per events and the number of strip per cluster are represented.

Once the Latency has been set, one can explore different radioactive sources with energies in the EASY range. Figures 4.27a and 4.27b show the charge collection in ADCs and converted into energy for an encapsulated Am-241 source (the encapsulation absorbs the beta emission). The Am-241 emits gamma rays of 60KeV (Data) energy, the spectrum reconstructed on Figure 4.27b is very coherent with the expected value. From Figure 4.27c we can appreciate that the trigger efficiency is lower than for the Sr-90 source and that the gamma typically induce signal in only one strip.

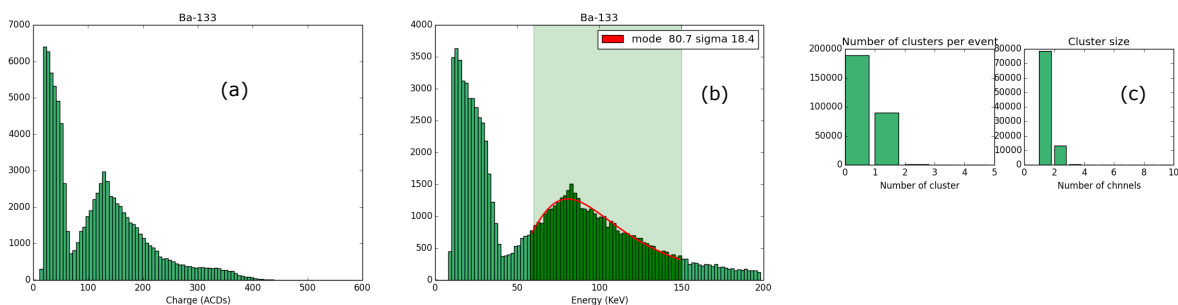


Figure 4.28.- Charge collected from Ba-133 source in ADC counts (a) and in energy (b). On (c), the number of cluster per events and the number of strip per cluster are represented.

The EASY system can also evaluate more complicated spectrums. For instance, the Ba-133 source emits mainly gammas of 81KeV and 302KeV, X-rays at 31KeV and betas to 80KeV and 133KeV. The results for Ba-133 are presented in Figure 4.28, the betas are seen as the betas from the Sr-90 (mainly *MIPS*), which is a distribution peaking at around

130 ADC counts (about 80KeV). On top of this distribution we can appreciate the pick of the 81KeV gammas. The 31KeV X-rays are also seen overlapping with the noise tail.

The system can also record the charge from cosmic muons, for that, the *Delay* on the DAQ configuration menu (section 3.4.2, Figure 3.9) has to be increased to deal with the low data rate, for example set the *Delay* to 600. Figure 4.29 corresponds to 14.973 cosmic rays recorded over 18hours and 14 minutes (0,23Hz data acquisition frequency, i.e. 13.7 cosmic rays/minute). Cosmic rays are mainly composed by *MIPs*. The distribution of strips in the cluster (Figure 4.29c) proves that the cosmic rays cross the sensor volume. Examining the hit map during data acquisition one can differentiate cosmic rays (flat distribution) from radioactive sources (similar to a Gaussian distribution).

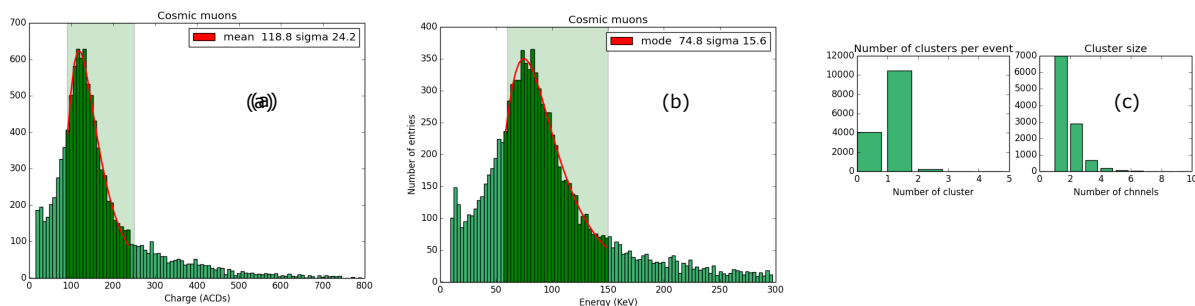


Figure 4.29.- Charge collected from Cosmic muons in ADC counts (a) and in energy (b). On (c), the number of cluster per events and the number of strip per cluster are represented.

The cosmic rays are always present and constitute part of the background of our experiments. If a low activity source is used, this background has to be taking into account. Figure 4.30 shows the data taken with a low activity Cs-109 source. Cs-109 emits 88KeV gammas and 21-22KeV X-rays. To accumulate enough data *Alibava-gui* has been running for 17 hours, then the cosmic ray spectrum is over imposed to the 88Kev gamma peak. Only the X-ray peak can be partially observed because of the overlap with the electronic noise.

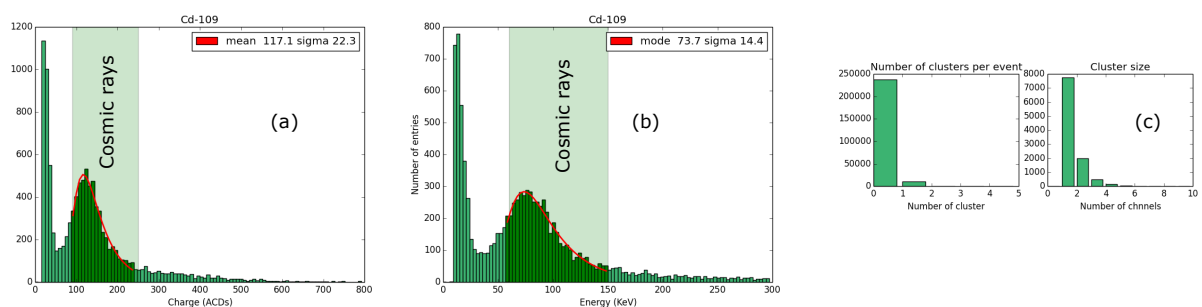


Figure 4.30.- Charge collected from low activity Cd-133 source in ADC counts (a) and in energy (b). On (c), the number of cluster per events and the number of strip per cluster are represented. Notice the large background from comic rays.

EXERCISE 10

SPECTROSCOPY USING SELF-TRIGGER

- Connect the flat cable between the Control Unit and the Sensor Unit (Section 1.2).
- Connect the USB cable between the Computer and the Control Unit (Section 1.2).
- Connect the LEMO cable between the Self-trigger output of the Sensor Unit and the Single trigger jack of the Control Unit (Section 1.2).
- Power the Control Unit (Section 1.2).
- Set detector bias voltage to 110V.
- Start *Alibava-gui* (Section 3.2).
- Select the Pulse trigger using:
 - Selecting *Pulse In* trigger (section 3.4.4, Figure 3.13)
 - Set trigger threshold *Thrs+ Trigger Pulse In* and *Thrs- Trigger Pulse In* to 500mV and -500mV (section 3.4.4, Figure 3.13).
- Place a Sr-90 source ion the carbon fibre rectangle of the Sensor Unit and select the Radioactive Source position of the Sensor Unit.
- Start the data acquisition and scan several Latency values for 128 forward
- Select the latency for which the charge value obtained is close to the one obtains with the Diode trigger (EXERCISE 5).
- Place the gamma or beta source you want to study (take notice available energy range of the EASY system: 20 to 300KeV)
- Take a calibration run: delay and charge (section 3.3.1), saving the calibration curve.
- Write an analysis program to extract the charge deposition (see EXERCISE 2 and 3), including:
 - Reading Pedestals form the data file (estimated during data acquisition).
 - Calculate common mode noise for each event. This will be done as in EXERCISE 2, but without taking into account the strips with signal. In order to do this, calculate for every event the mean charge of all channels. Identify the channels with a charge value of more than 3 standard deviations from the mean. Finally, calculate again the mean charge without those channels. This will give you the common mode of the event.
 - Define a Noise to signal cut and develop a cluster algorithm.
 - Obtaining the charge deposition adding the charge of the channels in a cluster.
 - Convert the charge in ADC counts to energy using the calibration curve.
 - Fitting the charge distribution to a Moyal function and obtain the most probable charge.
 - Calculate the charge deposition.
- Take a cosmic run. Take data without radioactive source and increasing the *Delay* on the DAQ configuration menu (section 3.4.2, Figure 3.9) to 100.
- Evaluate your cosmic background on the data taking with radioactive sources.
- Compare the data of different radioactive source: energy collected and cluster size.
- Interpret the energy reconstructed and the profile of the cluster size for different gamma/beta sources, betas for Sr-90 and cosmic ray data.

BIBLIOGRAPHY

Abt, I. et al. «Characterization of Silicon Microstrip Detectors Using an Infrared Laser System.» Nucl. Instr. Meth. A 423 (199): 303-319.

ALIBAVA Collaboration. «A portable readout system for microstrip silicon sensors.» IEEE Trans.Nucl.Sci. Vol. 56 (2009): 1642-1649,.

Bichsel, H. et al. Passage of particles through matter. <<http://pdg.lbl.gov/2011/reviews/rpp2011-rev-passage-particles-matter.pdf>>.

CERN. <http://home.web.cern.ch/>.

Data, Nuclear. <http://nucleardata.nuclear.lu.se/toi/perchart.htm>.

DESY. <http://www.desy.de/>.

Fermilab. www.fnal.gov/.

Kittel, C. Introduction to Solid State Physics, volume 8th Edition. John Wiley & Sons, 2005.

Löchner, S y Schmelling, M. The Beetle Reference Manual - chip version 1.3, 1.4 and 1.5. Max Planck Inst.: LHCb-2005-105 ; CERN-LHCb-2005-105, s.f.

Leo, W. R.: Techniques for Nuclear and Particle Physics Experiments: A How-to Approach, volume 2nd Edition. Springer-Verlag, 1987.

Lide, D. R.: Handbook of Chemistry and Physics. Editor-in-Chief, 77th Edition., 1996.

Lutz, G. Semiconductors Radiation Detectors, volume 2nd Edition. Springer, 1999.

Mante, J. «The Beta Ray Spectrum and Average Energy of Several Isotopes of Interest in Medicine and Biology.» Int. J. Appl. Radiat. Isotopes 23 (1972): 407.

Moyal, J. E.: «Theory of ionization fluctuation.» Phil. Mag. 56 (1955): 262.

Sze, S. M. Physics of Semiconductor Devices, volume 2nd Edition. Wiley Interscience, s.f.

The HDF group. HDF5-1.8.14. <<http://www.hdfgroup.org/HDF5/>>.